

## 1 **Context dependent activity of p63-bound gene regulatory elements**

2 Abby A. McCann<sup>1,2</sup>, Gabriele Baniulyte<sup>1,2</sup>, Dana L. Woodstock<sup>1</sup>, Morgan A. Sammons<sup>1,3</sup>

3

4 1) Department of Biological Sciences and The RNA Institute

5 University at Albany, State University of New York.

6 1400 Washington Ave, Albany, NY 12222

7

8 2) *Authors contributed equally*

9 3) *Corresponding Author: [masammons@albany.edu](mailto:masammons@albany.edu)*

10

### 11 **ABSTRACT**

12

13 The p53 family of transcription factors regulate numerous organismal processes including the  
14 development of skin and limbs, ciliogenesis, and preservation of genetic integrity and tumor  
15 suppression. p53 family members control these processes and gene expression networks  
16 through engagement with DNA sequences within gene regulatory elements. Whereas p53  
17 binding to its cognate recognition sequence is strongly associated with transcriptional activation,  
18 p63 can mediate both activation and repression. How the DNA sequence of p63-bound gene  
19 regulatory elements is linked to these varied activities is not yet understood. Here, we use  
20 massively parallel reporter assays (MPRA) in a range of cellular and genetic contexts to  
21 investigate the influence of DNA sequence on p63-mediated transcription. Most regulatory  
22 elements with a p63 response element motif (p63RE) activate transcription, with those sites  
23 bound by p63 more frequently or adhering closer to canonical p53 family response element  
24 sequences driving higher transcriptional output. The most active regulatory elements are those  
25 also capable of binding p53. Elements uniquely bound by p63 have varied activity, with p63RE-  
26 mediated repression associated with lower overall GC content in flanking sequences.  
27 Comparison of activity across cell lines suggests differential activity of elements may be  
28 regulated by a combination of p63 abundance or context-specific cofactors. Finally, changes in  
29 p63 isoform expression dramatically alters regulatory element activity, primarily shifting inactive  
30 elements towards a strong p63-dependent activity. Our analysis of p63-bound gene regulatory  
31 elements provides new insight into how sequence, cellular context, and other transcription  
32 factors influence p63-dependent transcription. These studies provide a framework for  
33 understanding how p63 genomic binding locally regulates transcription. Additionally, these  
34 results can be extended to investigate the influence of sequence content, genomic context,  
35 chromatin structure on the interplay between p63 isoforms and p53 family paralogs.

36

### 37 **INTRODUCTION**

38

39 Transcription factors regulate gene expression networks during development and are  
40 responsible for the maintenance of cellular and organismal homeostasis. These activities  
41 require transcription factor interactions with DNA, usually via conserved sequence motifs within  
42 cis-regulatory elements (CRE) like promoters and enhancers (Slattery et al., 2014). Sequence  
43 specific transcription factor binding to regulatory elements can affect gene expression in  
44 multiple, context-dependent ways, including direct recruitment of cofactors or RNA polymerase

45 and through control of local and long-distance chromatin structure. TF control of gene  
46 expression is not a binary “on/off” state, and represents a range of dynamic interactions with  
47 DNA dictated by sequence, chromatin, and other locally-bound transcription factors (Hager et  
48 al., 2009; Ricci-Tam et al., 2021). Ultimately, understanding how DNA sequence and chromatin  
49 context at CREs controls TF binding is critical for dissecting complex gene regulatory networks  
50 during development and in disease.

51  
52 The tight relationship between sequence-specific transcription factor activity, CREs, and gene  
53 expression is especially important for lineage specification during development (Spitz and  
54 Furlong, 2012; Long et al., 2016; Barral and Zaret, 2023). The transcription factor p63, a  
55 member of the well-known p53 family, is a key regulator of epithelial lineage specification and  
56 self-renewal (Senoo et al., 2007; Melino et al., 2015; Li et al., 2023). Extensive work using p63  
57 loss-of-function mouse models demonstrates the essentiality of p63 for development of limbs,  
58 digits, and craniofacial structures (Yang et al., 1998; Mills et al., 1999). These phenotypes are  
59 consistent with those in humans, where p63 mutations cause multiple disorders rooted in  
60 epithelial cell dysfunction, including EEC (Ectrodactyly, Ectodermal Dysplasia and Cleft lip or  
61 Cleft lip and palate), Limb-Mammary Syndrome (LMS), Rapp-Hodgkin Syndrome (RMS), and  
62 ADULT syndrome (Celli et al., 1999; Amiel et al., 2001; McGrath et al., 2001, 2001; van  
63 Bokhoven et al., 2001; Bougeard et al., 2003). These epithelial-associated activities underlie the  
64 importance of p63 in multiple organ systems during development and in post-development  
65 contexts (Fletcher et al., 2011; Yallowitz et al., 2014; Richardson et al., 2017; Song et al., 2018).  
66 Organismal-level phenotypes in mouse models and human disorders are consistent with the  
67 indispensable role of p63 in the formation and maintenance of both the epidermis and epithelial-  
68 derived cells and tissues.

69  
70 Mutations within p63-bound CREs are also directly linked to human developmental disorders,  
71 suggesting p63 regulation of CREs is required for development (Rahimov et al., 2008;  
72 Thomason et al., 2010; Lin-Shiao et al., 2019). While multiple human disorders are linked to  
73 mutations that reduce p63 function, p63 hyperactivity and gain-of-function contribute to post-  
74 developmental disorders like cancer. Overexpression of p63 drives tumorigenesis in squamous  
75 cell carcinomas (Ramsey et al., 2013; Saladi et al., 2017; Abraham et al., 2018), while genetic  
76 rearrangements in *TP63* lead to gain-of-function activities of p63 fusion proteins important for  
77 lymphoma progression (Saladi et al., 2017; Ng et al., 2018; Moses et al., 2019; Wu et al., 2023,  
78 p. 63).

79  
80 Like other transcription factors, p63 activity requires direct binding to specific DNA motifs within  
81 CREs (Yang et al., 2006; Perez et al., 2007; Lambert et al., 2018). The *TP63* gene encodes  
82 multiple transcript and protein isoforms (Mills et al., 1999; Candi et al., 2006; Murray-Zmijewski  
83 et al., 2006; Sethi et al., 2015; Marshall et al., 2021; Osterburg and Dötsch, 2022), with the two  
84 most prominent being TAp63 $\alpha$  and  $\Delta$ Np63 $\alpha$  generated from alternative promoter usage. TAp63 $\alpha$   
85 is an obligate transcriptional activator, and functions in preservation of genetic integrity in germ  
86 cells, adult stem cell maintenance, and late-stage keratinocyte differentiation (Candi et al., 2006;  
87 Su et al., 2009; Gebel et al., 2017). On the other hand,  $\Delta$ Np63 $\alpha$ 's activity is strongly context-  
88 dependent, and has been shown to be both a transcriptional activator and repressor (Fisher et

89 al., 2020).  $\Delta$ Np63 $\alpha$  is a pioneer factor which licenses epithelial-specific regulatory elements  
90 during development (Pattison et al., 2018; Li et al., 2019; Lin-Shiao et al., 2019; Yu et al., 2021),  
91 but can also bookmark chromatin structure at already established active regions or control 3D  
92 interactions to repress gene expression (Bao et al., 2015; Pattison et al., 2018).  $\Delta$ Np63 $\alpha$  can  
93 also locally recruit traditional co-activators, like SMAD proteins and p300 (Krauskopf et al.,  
94 2018; Katoh et al., 2019; Klein et al., 2020, p. 300; Sundqvist et al., 2020), or co-repressors, like  
95 HDACs (LeBoeuf et al., 2010; Ramsey et al., 2011), to regulatory elements to variably control  
96 transcription (Sethi et al., 2014). The specific temporal and spatial contexts where  $\Delta$ Np63 $\alpha$   
97 performs these various transcriptional roles, and how these differential activities are regulated,  
98 remain unclear.

99  
100 Gene regulatory elements contain multiple transcription factor binding sites in particular  
101 orientations that “code” for specific transcriptional outcomes. The combination of local sequence  
102 context and transcription factor occupancy at regulatory elements ultimately controls gene  
103 expression networks and vast cell fate decisions (Kulkarni and Arnosti, 2003; Zaret and Mango,  
104 2016; Halfon, 2020). We implement STARR-seq MPRA technology to address whether  
105 sequence content and context of p63-bound gene regulatory elements might explain differential  
106 p63 activities like transcriptional activation or repression (Arnold et al., 2013). We identified  
107 sequence features within and around p63 binding sites that influence p63-specific activities.  
108 p63-mediated repression is most associated with local GC content and the presence of nearby  
109 motifs for known transcriptional repressors. p63-mediated activation is influenced by specific  
110 classes of p63 response element (RE) DNA motifs that also permit binding by p53. p63-bound  
111 CRE activity changes across different epithelial cell contexts with this variation potentially  
112 regulated by changes in p63 expression and flanking transcription factor motifs.  $\Delta$ Np63 $\alpha$   
113 occupancy is only weakly correlated to transcriptional output unlike strong transactivators like  
114 p53. However in the context of expression of a different isoform of p63, TAp63 $\beta$ , transcriptional  
115 activation greatly increases, suggesting that isoform switching is a mechanism that controls the  
116 activity of p63-bound regulatory elements.

117

## 118 **RESULTS**

119

### 120 ***Examination of the transcriptional regulatory potential of p63-bound elements***

121

122 To explore how  $\Delta$ Np63 $\alpha$ , hereby referred to as p63, controls epithelial gene regulatory  
123 networks, we measured transcriptional activity of putative cis-regulatory elements (CRE) bound  
124 by p63 using a massively parallel reporter assay (MPRA). We selected candidate CREs from a  
125 recent meta-analysis examining p63 ChIP-seq binding across multiple human epithelial-derived  
126 cell lines (Riege et al., 2020) and cloned them into a reporter system using the STARR-seq  
127 strategy (Muerdter et al., 2018; Neumayr et al., 2022)(Fig. 1A). We selected candidate CREs  
128 where p63 binding was observed in at least 8 independent ChIP-seq experiments, resulting in  
129 17,310 elements. Sequences were cloned from single-stranded oligo pool where the likely p63  
130 response element (p63RE) was placed in the center of the oligo, flanked by up to 52 nucleotides  
131 on either side of genomic context depending on the length of the identified p63RE. To  
132 understand the specific role of p63 in transcriptional regulation by the selected CREs, we

133 created two variants predicted to disrupt p63 binding. We performed conservative substitutions  
134 of nucleotides enriched at any single position with greater than 80% frequency (p63RE mut)  
135 (Fig. 1B, Table S1). We also performed a random nucleotide shuffle of the predicted p63RE  
136 located at the center of the CRE as a control for disrupted p63 binding (p63RE shuffle). Finally,  
137 nucleotides flanking the p63RE (p63RE flank) or the entire CRE (full shuffle) were shuffled, all  
138 while preserving GC content of the original CRE sequence. The sequence of all variants can be  
139 found in Table S1.

140  
141 We next examined the genomic and chromatin context of these elements to better understand  
142 how these characteristics might relate to their observed transcriptional output. Although many  
143 p63 binding events are intragenic (Fig. 1D), less than 20% of those are within 5kb of the  
144 transcriptional start site (TSS). Most sites are localized over 5kb from the TSS suggesting  
145 potential function as distal regulatory elements (Fig. 1C). ENCODE candidate Cis-Regulatory  
146 Element (cCRE) classification suggests that most of these p63-bound regions display distal  
147 enhancer-like signatures characterized by accessible chromatin and stereotypical histone  
148 modifications such as enrichment of H3K27ac and lack of H3K4me3 (Fig. 1E) (Moore et al.,  
149 2020). The next largest group overlaps the cCRE designation of NA which includes both  
150 heterochromatin and “quiescent” chromatin lacking known chromatin-based features of  
151 regulatory DNA. On average, 80% of these p63-bound elements are found in open chromatin  
152 regions of basal epithelial cell types (Fig. 1F) (Thurman et al., 2012; Sheffield et al., 2013). In  
153 contrast, most p63 binding sites are found in closed chromatin regions in all other cell types. We  
154 next examined the distribution of chromatin features surrounding our MPRA elements using  
155 chromHMM, which defines categorical chromatin states across multiple cell lines and conditions  
156 (Fig. 1G) (Ernst and Kellis, 2015; Vu and Ernst, 2022). In three p63-positive epithelial cell lines  
157 including the model mammary epithelial line MCF-10A, we observe enhancer-like enrichment at  
158 greater than 45% of the MPRA elements compared to an average of approximately 20% in non-  
159 epithelial cell lines (Fig. 1H). The epithelial specific enhancer-like chromatin features for the  
160 surveyed MPRA elements is consistent with epithelial lineage-restricted expression and pioneer  
161 factor activity of p63. We chose to use the model basal mammary epithelial cell line MCF-10A  
162 cell line for subsequent studies, as significant prior datasets for p63 occupancy, transcriptional  
163 regulation, and chromatin context are available. In line with summary statistics from ENCODE  
164 cCRE and chromHMM, the majority of our MPRA regions bound by p63 are enriched for  
165 H3K27ac and H3K4me2, but depleted for H3K4me3 (Fig. 1I), suggesting these elements have  
166 primarily enhancer-like qualities in MCF-10A.

167  
168 We then assayed the activity of these p63-bound CRE to investigate sequence requirements for  
169 p63-dependent transcription in MCF-10A. Under basal conditions, these cells primarily express  
170 the p63 isoform  $\Delta Np63\alpha$ , which is a context-dependent transcriptional activator or repressor  
171 (Fisher et al., 2020). We performed two biological replicates by transfecting the STARR-seq  
172 p63RE library into MCF-10A, isolated total RNA, and then specifically amplified and deep  
173 sequenced the self-transcribed CRE. Plasmid DNA pools were also sequenced as a  
174 transfection control, and CRE-driven RNA expression was quantified as a ratio of RNA:DNA.  
175 While 17,310 candidate p63-bound CREs were originally selected for analysis, synthesis,  
176 cloning, and experimental dropout reduced the number of regions used in downstream

177 experiments and analysis to 13,696. We only included regions where all five variants were  
178 found in the DNA and RNA libraries at sufficient depth (Table S2, Materials and Methods).

179  
180 First, we examined the role of the p63RE in mediating transcriptional activity. Mutation of either  
181 the entire p63RE (RE shuffle) or of specific nucleotides predicted to be critical for p63 binding  
182 (RE mut) substantially reduced transcriptional activation ( $p \leq 1.00e-04$ ) (Fig. 1J). Similar  
183 reductions in activity were seen when the entire CRE was shuffled, as expected by the loss of  
184 all native transcription factor binding sites. On the contrary, shuffling DNA sequence flanking the  
185 p63RE, and thus disrupting binding of other transcription factors, did not dramatically affect  
186 CRE-mediated transcription. These data suggest p63-bound CREs are more dependent on the  
187 central p63RE for transcriptional activation than other potential TF binding sites in flanking  
188 genomic context, similar to previous observations of the central importance for the p53 family  
189 RE at regulatory elements (Janky et al., 2014; Verfaillie et al., 2016; Sahu et al., 2022).

190

### 191 ***Influence of p63 and p53 occupancy on cis-regulatory element activity***

192

193 Given the importance of the central p63RE on CRE activity, we next investigated how p63  
194 occupancy and enrichment at these elements influences transcriptional activity. We initially  
195 selected p63-bound regions for study that were identified in a meta-analysis of p63 ChIP-seq  
196 binding in between 8 and 20 independent ChIP-seq studies from different epithelial cell types,  
197 but did not contain p63 binding data from MCF-10A (Riege et al., 2020). We therefore used  
198 MCF-10A p63 ChIP-seq data from a prior study to examine how *in vivo* p63 enrichment was  
199 linked to CRE activity (Karsli Uzunbas et al., 2019). Increasing p63 enrichment in MCF-10A  
200 cells corresponds with increased p63 occupancy across epithelial cell types (Fig. 2A). In  
201 general, more ubiquitous p63 occupancy across cell types relates to p63 enrichment in MCF-  
202 10A, although significant variation exists across the range of binding events (Fig. 2A). CREs are  
203 more active when p63 binding occupancy is more ubiquitous compared to sites where p63  
204 binding is restricted or cell-line dependent (Fig. 2B). On the contrary, MPRA activity is poorly  
205 correlated with p63 ChIP-seq enrichment in MCF-10A cells (Fig. 2C, Spearman  $\rho=0.127$ ).  
206 These observations suggest that ubiquitous p63 binding, those events observed across many  
207 cell types, is more closely linked with transcriptional output than p63 binding enrichment as  
208 measured by ChIP-seq.

209

210 Many p63 binding sites are shared by its family member p53, which is a near universal  
211 transactivator (Fischer et al., 2014; Sahu et al., 2022). Prior p63 ChIP-seq meta-analyses  
212 identified distinct p63 response element (RE) classes that differ primarily in their ability to  
213 support binding of p53 (p53RE+p63RE) or p63 only (unique p63RE) (Riege et al., 2020).  
214 Therefore, we examined whether intrinsic differences in p63RE motifs and overlapping binding  
215 with p53 might better reflect the observed transcriptional activity. CREs containing the  
216 p53RE+p63RE motif type were significantly more active than those with a unique p63RE (Fig.  
217 2D), and saw a greater drop in activity when the central motif was lost. Similar to p63, p53  
218 binding observations correlate with transcriptional output (Fig. 2B,E). Unlike our observations  
219 with p63, p53 binding strength from MCF-10A cells is better correlated with CRE activity (Fig.  
220 2F, Spearman's  $\rho = 0.405$ ).

221  
222 We next measured MPRA activity in MCF-10A *TP53*<sup>-/-</sup> cells (Fig. 2G) to parse specific  
223 contributions of p53 versus p63. CRE activity is significantly reduced in *TP53*<sup>-/-</sup> relative to WT  
224 MCF-10A cells (Fig. 2H). However, we also observe an additional significant reduction in activity  
225 when the central p63RE is mutated in *TP53*<sup>-/-</sup> conditions. Notably, in aggregate, p53RE+p63RE  
226 elements are more active than unique p63 CREs even in the absence of p53 (Fig. 2I). These  
227 data suggest that although p53 drives a substantial proportion of transcriptional activity for these  
228 CREs, p63 still functions as an activator at p53RE+p63RE motifs even in p53s absence. They  
229 also suggest that inherent sequence differences may contribute to differential transcriptional  
230 output of p63-bound CREs.

### 231 232 ***Intrinsic response element sequence differences and GC content contribute to p63 and*** 233 ***p53-dependent transcriptional activity***

234  
235 Initial analysis suggests that p63 primarily functions as a transcriptional activator, with mutations  
236 to the p63RE significantly reducing transcriptional output (Fig. 1J) despite p63 enrichment being  
237 poorly correlated with transcriptional activity (Fig. 2C). CREs containing p53RE+p63RE  
238 sequences are substantially more active than those containing motifs supporting only p63  
239 binding (Fig. 2D) independent of whether p53 or p63 is engaged (Fig. 2I). The extent to which  
240 variation in half-site sequence and other intrinsic DNA information within a p53 family response  
241 element leads to differential binding kinetics and activities remains an open question in the field  
242 (Szak et al., 2001; Safieh et al., 2023).

243  
244 p53RE+p63RE motifs were originally subdivided into five categories based on differences in  
245 occupancy and abundance in p53/p63 ChIP-seq datasets: primary, secondary, tertiary,  
246 quaternary, and quinary (Fig. 3A) (Riege et al., 2020). Primary motifs are considered the  
247 canonical p53 family motif, containing two canonical CWWG half-sites separated by a 6bp  
248 spacer (el-Deiry et al., 1992; Castro-Mondragon et al., 2022). CREs containing these elements  
249 support higher enrichment of p63 (Fig. 3B) and p53 (Fig. 3C) and are more active (Fig. 3D)  
250 compared to the other classes. The activity of secondary, quaternary, and quinary elements  
251 descend in that order (Fig. 3D), as do p63 and p53 occupancy (Fig. 3B,C). CRE activity  
252 significantly decreases when nucleotides critical for p53/p63 binding are mutated in both primary  
253 and secondary motifs (Fig. 3D). Because we selected CRE sequences based on p63  
254 occupancy alone, our assays ultimately did not contain any tertiary p53RE+p63RE motifs.  
255 Likely due to their limited number in this dataset, mutation of quaternary (n=50) and quinary  
256 (n=82) motifs lead to a small, but not statistically significant, decrease in CRE activity (Fig. 3D).  
257 Similar to p53, p63 activates both primary and secondary motif-containing elements, but without  
258 a strong preference for primary motifs (Fig. 3E).

259  
260 We next examined whether CRE activity might relate to specific classes of the unique p63RE  
261 motifs (Fig. 3F). The primary and tertiary motifs resemble canonical p53 family motifs, with two  
262 half sites separated by a 6bp spacer. Secondary, quaternary, and quinary motifs are  
263 characterized by the presence of a single half-site coupled with an incomplete second half-site.  
264 Senary motifs, relatively lowly represented in the test sequences, generally contain a single,

265 weak half-site. Septenary motifs were excluded from this analysis due to low representation  
266 (n=2). The relationship between unique p63RE motif type and CRE activity is more nuanced  
267 than for those with p53RE+p63RE motifs. p63 enrichment is highest at primary and quaternary  
268 elements (Fig. 3G), but tertiary elements drive the highest level of CRE expression (Fig. 3H,I).  
269 Loss of the central element leads to statistically significant loss in CRE activity for primary,  
270 secondary, tertiary, and quaternary elements, with quinary and senary motifs driving the lowest  
271 expression and having the least dependence on the central motif. These observations are  
272 similar in the presence and absence of p53 consistent with lack of p53 binding at these sites  
273 (Fig. 3I)

274  
275 Increasing p63 ChIP-seq enrichment is not coupled to increased activity (Fig. 2C), and different  
276 p63RE classes contribute to, but do not explain, differential CRE activity. We sought to  
277 determine whether other local sequence features might provide additional insight into p63-  
278 dependent CRE activity. Previous studies demonstrate dinucleotide repeat motifs (DRMs) are  
279 an indicator of regulatory sequence activity (Yanez-Cuna et al., 2012; White et al., 2013;  
280 Colbran et al., 2017). Dinucleotide content was generally similar within CRE classes with the  
281 exception of increased GC and CG DRM enrichment in unique p63RE and increased AT and  
282 TA enrichment for p53RE+p63RE (Fig. 3J). Increased AT and TA dinucleotide content in the  
283 p53RE+p63RE likely reflects the strong preference of p53 for these dinucleotides in half-sites  
284 (Fig. 3A,3J). CG dinucleotide enrichment and subsequent methylation could potentially explain  
285 reduced activity of unique p63RE compared to p53RE+p63RE, but these observations require  
286 further study.

287  
288 Differences in the distribution of dinucleotides led us to ask whether overall GC content might  
289 vary between the two p63RE motif classes, as increasing GC content is linked to increased  
290 activity of regulatory elements (Colbran et al., 2017; Lecellier et al., 2018). Unique p63RE have  
291 higher overall GC content and these differences are primarily in regions flanking the central  
292 p63RE (Fig. 3K). CREs containing p53RE+p63RE motifs are more active despite lower overall  
293 GC content relative to unique p63RE. We observe a strong trend between increasing GC  
294 content and increasing CRE activity for p53RE+p63RE in the absence of p53 (Fig. 3E,M), which  
295 is not observed when p53 is present (Fig. 3D,M). For unique p63 motifs, CRE activity (Fig. 3H,I)  
296 closely matches trends in GC content in WT and *TP53*<sup>-/-</sup> conditions (Fig. 3L), perhaps  
297 suggesting increased GC content between elements can overcome the absence of a strong  
298 transactivator like p53.

299  
300 Taken together, these data suggest that specific classes of p63REs lead to modest differences  
301 in p63-dependent CRE transcriptional output. These observations suggest that for elements  
302 regulated by p53, motif type and p53 occupancy/affinity are important determinants of high  
303 transactivation relative to other sequence-intrinsic features, like GC content. On the contrary,  
304 these elements are p63-dependent, but increased p63 enrichment and p63RE motif features do  
305 not directly result in higher transactivation.

306  
307 ***Local sequence content and co-occurring transcription factor motifs are associated with***  
308 ***differential p63-dependent activation and repression***

309  
310 Our data suggest additional intrinsic DNA sequence characteristics like GC content contribute to  
311 maximal activity of p63-bound elements beyond those that directly affect recruitment of p63.  
312 p53-bound elements are more active and DNA motifs with higher occupancy lead to higher  
313 overall transcriptional output. Our data suggest that loss of p63 binding via mutation of the  
314 central p63RE leads to a marked decrease in CRE-driven transcriptional activity. When viewed  
315 in aggregate, these results suggest p63 predominantly activates transcription. The  $\Delta$ Np63 $\alpha$   
316 isoform of p63, which is the predominant isoform in basal epithelial cells like MCF-10A,  
317 mediates both transcriptional activation and repression, along with chromatin remodeling  
318 activities, when binding to regulatory sequences (Bao et al., 2015; Fisher et al., 2020; Yu et al.,  
319 2021). We asked whether p63 and p53 transcriptional activation might mask other context  
320 dependent activities like repression by examining CRE behavior in the absence of p53. We  
321 classified p63-dependent CRE activity as “activating” if mutation of the p63RE led to lower  
322 activity relative to WT and “repressing” if lack of p63 binding led to more transcriptional output.  
323 Overall, we observe p63-dependent transcriptional activation at nearly 30% (4044/13696) of  
324 CREs and repression at only 10% (1345/13696) (Fig. 4A). Interestingly, the activity of most p63-  
325 bound elements is not affected when the central p63RE is mutated, regardless of motif type  
326 (Fig. 4A). These data potentially suggest that either p63 has non-transcriptional roles that  
327 cannot be measured via STARR-seq-style reporter assays or that these elements are strongly  
328 cell-type or context-dependent.

329  
330 Activities varied based on the type of p63RE motif found within the CRE. Those containing a  
331 p53RE+p63RE motif are almost twice as likely to require p63 for transcriptional activation (Fig.  
332 4A). Primary p53RE+p63RE motifs more frequently lead to p63-dependent activation compared  
333 to any other class whereas p63-mediated repression is generally similar across subclasses of  
334 p63 response elements (Fig. 4B). Activation at unique p63RE sites is relatively similar across  
335 motif types with the exception of those containing quaternary motifs (Fig. 4C). Because they are  
336 found in only 65 total regulatory elements, we expect that quaternary motifs are unlikely to  
337 broadly represent a general feature that underlies p63-dependent transcriptional activation. GC  
338 content spanning the central p63RE is slightly reduced in p63-repressed elements relative to  
339 those where p63 activates transcription (Fig. 4D). p63RE type and nucleotide content partially  
340 reflect differences between p63-mediated activation and repression, although these effects are  
341 relatively modest. Therefore, our data suggest the p63RE motif is critical, but that variation in  
342 sequence content between elements is not a major determinant in p63-dependent  
343 transcriptional activation and repression.

344  
345 Cis-regulatory element activity is controlled by the total complement of transcription factors and  
346 co-factors interacting with the element (Kulkarni and Arnosti, 2003; Jindal and Farley, 2021). We  
347 asked whether sequences, and therefore other DNA binding factors, flanking the central p63RE  
348 motif might contribute to activation or repression of p63-bound CREs. As expected, mutation of  
349 the central p63RE led to decreased activity at p63-activated elements and an increase in activity  
350 at p63-repressed elements, indicative of p63-dependent activity (Fig. 4E). Shuffling sequences  
351 flanking the central p63RE led to partial loss of function for both p63-activated and repressed  
352 elements. These data suggest that DNA sequences outside of the central p63RE contribute to

353 p63-mediated activities, but the specific mechanisms are not known. We then explored if  
354 particular transcription factor motifs might be enriched in CREs where p63 activity was either  
355 activating or repressing (Fig. 4F). We used p63RE-containing elements whose activity was p63-  
356 independent (unchanged) as the background control to specifically identify unique motifs that  
357 might contribute to either activation or repression versus general enrichment with p63RE. p53  
358 family motifs are enriched in activating elements, likely reflecting the observation that most  
359 activating elements contain the primary sub-motif which is most closely aligned with the  
360 canonical motif models used in the HOMER motif finding algorithm (Table S3) (Heinz et al.,  
361 2010; Duttke et al., 2019). Activating elements are also broadly enriched with AP-1 family motifs  
362 consistent with these elements supporting transcriptional activation (Biddie et al., 2011;  
363 Thurman et al., 2012; Seo et al., 2021). Elements repressed by p63 lack these canonical trans-  
364 activator motifs, but are enriched for a series of known transcriptional repressors like Snail,  
365 Slug, Zeb1, and Zeb2. All four of these factors have established roles in transcriptional  
366 repression during epithelial-to-mesenchymal transition (Peinado et al., 2007; Kalluri and  
367 Weinberg, 2009; Pastushenko and Blanpain, 2019). p63-repressed elements are also enriched  
368 for motifs for a select set of lineage-specific transcription factors such as Ascl2, MyoG, Tbx5,  
369 and Pitf1a, perhaps suggesting p63 and these factors might cooperate to repress key elements  
370 during lineage transitions during directed differentiation (Pattison et al., 2018; Li et al., 2019).  
371 Although motifs for known activators and repressors are enriched in flanking regions of p63-  
372 bound CREs with specific activities, we cannot rule out that DNA shape or p63RE-adjacent  
373 context might contribute to changes in p63 binding and activity as they do for p53 (Senitzki et  
374 al., 2021; Safieh et al., 2023).

### 375 376 ***Cell identity and isoform availability influence p63-bound cis-regulatory element activity***

377  
378 Our data indicate that most p63-bound CREs are not dependent on p63 for their transcriptional  
379 activity in MCF-10A STARR-seq assays (Fig. 4A). p63 is a context-dependent transcriptional  
380 activator and repressor whose activity is restricted to epithelial cells. While broadly important as  
381 a regulator of lineage specification and self-renewal, p63 activity varies across epithelial cell  
382 types. For example, p63 is amplified in many squamous cell carcinomas and is associated with  
383 poor prognosis and pro-tumorigenic phenotypes (Latil et al., 2017; Saladi et al., 2017; Abraham  
384 et al., 2018). We therefore asked whether p63 expression across different epithelial contexts  
385 might lead to differential activity of p63-bound CREs in our assay. HaCaT are a spontaneously  
386 immortalized keratinocyte line that can undergo squamous differentiation in culture and  
387 preserve many of the features of normal human keratinocytes (Wilson, 2013). SCC-25 are  
388 squamous cell carcinoma of the tongue, a cancer type that is highly-dependent on p63 for  
389 proliferation (Thurfjell et al., 2005; Latil et al., 2017; Saladi et al., 2017; Pokorna et al., 2022).  
390 Importantly, both cell lines have inactivating mutations in p53 that limit the analysis to p63-  
391 dependent activities (Bamford et al., 2004). HaCaT and SCC-25 also express higher levels of  
392 p63 than MCF-10A cells (Fig. 5A) (Sethi et al., 2015), allowing us to ask whether increasing  
393 cellular p63 concentration might alter CRE activity.

394  
395 We transfected the MPRA library into either HaCat or SCC-25 cell lines and measured  
396 transcriptional output as previously described. Due to differences in transfection efficiency

397 between cell types, we ultimately recovered 8,566 elements with paired WT and mutant  
398 expression data across all replicates of MCF-10A *TP53*<sup>-/-</sup>, HaCaT, and SCC-25 cell lines. We  
399 asked whether variation in cell type or p63 expression levels might alter the scope of p63-  
400 dependent activation or repression. Overall, the percentage of p63-activated elements is similar,  
401 albeit slightly lower, in HaCaT and SCC-25 compared to MCF-10A. SCC-25 cells have nearly 3-  
402 fold more p63-repressed elements than the other cell lines (Fig. 5B) although we observe  
403 relatively few enriched transcription factor motifs that might contribute to this repression (Table  
404 S3). p63-dependent CRE activity varies across these three epithelial cell contexts as most  
405 CREs have varied activity across at least two cell lines (Fig. 5C). p63 expression is elevated in  
406 both HaCaT and SCC-25, although this does not appear to directly correlate with observed  
407 differences in CRE activity. Nearly 30% of CREs do not require the central p63RE for  
408 transcriptional activity in any condition (Fig. 5B,C), suggesting they function independent of p63.  
409 These results indicate that the collective action of p63 and other transcription factors might  
410 underlie the observed variability in gene regulatory element activity.

411  
412 We then focused on the cell line-specific variability in p63-mediated transcriptional activation.  
413 Slightly over 40% (988) of p63-activated CREs are shared between MCF-10A and SCC-25,  
414 leaving substantial variability in p63-dependent activity between CREs in SCC-25 (1,287) and  
415 MCF-10A (1,400). We therefore examined the differences in transcription factor motif  
416 enrichment between p63-dependent CREs in MCF-10A and SCC-25. AP-1 and TEAD family  
417 motifs are enriched at p63-activated CREs in both MCF-10A and SCC-25 consistent with their  
418 reported roles in transcriptional activation at regulatory elements (Fig. 5D) (Biddie et al., 2011;  
419 Currey et al., 2021; Seo et al., 2021). Ets, Smad, and C2H2 zinc finger-related motifs are  
420 uniquely enriched in MCF-10A, while SCC-25 p63-activated CREs are enriched for multiple  
421 unique transcription factor family motifs, including those from the GATA, FOX, Oct, and Maf  
422 families (Fig. 5E). While additional work is needed to determine the extent to which these  
423 putative transcription factors are involved, our results provide evidence that p63-dependent  
424 transcriptional activity is influenced by the activity of other transcription factors in a cell type-  
425 dependent fashion.

426  
427 Although specific elements shift between being activated or repressed by p63 depending on  
428 epithelial cell context, ultimately, p63 is still not required for activity of most p63-bound CREs  
429 (Fig. 5C). p53 and p63 share highly overlapping DNA response element motifs (el-Deiry et al.,  
430 1992; Perez et al., 2007; Riege et al., 2020), and p53 binding leads to near universal  
431 transcriptional activation due to the presence of a strong N-terminal transactivation domain  
432 (TAD) (Fischer et al., 2014; Verfaillie et al., 2016). Basal epithelial cells primarily express  
433  $\Delta$ Np63 $\alpha$  (Fig. 5A), but multiple N- and C-terminal isoforms of p63 can be expressed in different  
434 cellular contexts (Marshall et al., 2021). We therefore asked whether the p63-bound CRE  
435 activity might have p63 isoform-specific dependence. TAp63 isoforms are expressed in late  
436 stages of keratinocyte differentiation and are required for the response to genotoxic damage in  
437 germ cells (Koster et al., 2004; Truong et al., 2006; Beyer et al., 2011; Deutsch et al., 2011).  
438 TAp63 $\alpha$  drives high levels of transcriptional activation in a stimulus-dependent fashion (Deutsch  
439 et al., 2011; Coutandin et al., 2016), whereas other C-terminal isoforms, like TAp63 $\beta$  are  
440 constitutively active (Lena et al., 2021). We therefore chose to measure CRE activity in

441 response to expression of TAp63 $\beta$  in order to avoid potential crosstalk with genotoxic or other  
442 cell stress pathways. We transfected the MPRA library into MCF-10A cells where either a  
443 control protein (GUS) or TAp63 $\beta$  was expressed under doxycycline-inducible control (Fig. 5F).  
444 The distribution of p63-bound CREs in control conditions that are p63-activated, repressed, or  
445 independent is highly similar to our previous assays in MCF-10A and MCF-10A *TP53*<sup>-/-</sup> cell lines  
446 (Fig. 5H vs. Fig. 4A). TAp63 $\beta$  expression led to increased overall CRE activity and importantly,  
447 this activity is dependent on the central p63RE motif (Fig. 5G). Nearly 70% of CREs display  
448 p63RE-dependent transcriptional activation when TAp63 $\beta$  is expressed, more than a 2-fold  
449 increase compared to control conditions (Fig. 5H). This is most observable at CREs with unique  
450 p63RE which see a 3 fold shift towards p63-dependent transcriptional activation and a near-  
451 complete loss of repression in the presence of TAp63 $\beta$ . Taken together, these results suggest  
452 that context-dependent p63 isoform expression alters the activity of cis-regulatory elements and  
453 that TA-isoforms primarily activate transcription.

454

## 455 **Discussion**

456

457 The importance of p63 in regulating epithelial cell identity is supported by extensive genetic and  
458 biochemical evidence. p63 regulates epidermal development through its transcription factor  
459 activity and control of epithelial-specific transcription and chromatin structure. These activities  
460 require p63 binding and context-specific transcriptional regulation, but how DNA sequence at  
461 regulatory elements affects p63 activity is an open question. Here, we examine whether the  
462 sequence content and context of p63 binding sites controls p63-dependent transcriptional  
463 activity using massively parallel reporter assays. We find that sequence content of p63  
464 response element motifs influences p63 binding and transcriptional activity, but that this  
465 relationship is complicated. The complex relationship between sequence and function is partially  
466 due to p63 roles as both a context-dependent transcriptional activator and repressor.

467

468  $\Delta$ Np63-dependent repression is relatively rare compared to activation, as has been suggested  
469 by studies combining p63 binding and global transcriptome analyses (Riege et al., 2020).

470 Repression can be mediated by C-terminal recruitment of known co-repressors like histone  
471 deacetylases or through antagonism of other transcription factors, like p53 (LeBoeuf et al.,  
472 2010; Ramsey et al., 2011; Woodstock et al., 2021). Our data suggest that slight variation in  
473 p63RE motif sequence content, like varying GC and dinucleotide content, might partially explain  
474 varying activation or repression, but this is likely only a minor contributor. Motifs for known  
475 repressive transcription factors like Snail, Slug, Zeb1, and Zeb2 are specifically enriched in p63-  
476 repressed elements. Interestingly, these factors are key regulators of epithelial-to-mesenchymal  
477 transition (EMT) (Peinado et al., 2007), a process globally suppressed by p63 (Yoh et al., 2016;  
478 Latil et al., 2017). While they may antagonize each other globally, p63 and these EMT-  
479 promoting factors may have cooperative roles in repression of specific genes. p63 switches  
480 between repressive and activating states during development, starting by repressing non-  
481 epithelial lineage genes before switching to activation during epithelial commitment (Pattison et  
482 al., 2018; Santos-Pereira et al., 2019). p63 also locally represses some TFAP2C binding sites  
483 important for early epidermal specification during later stages of keratinocyte maturation (Li et  
484 al., 2019). Repression in these settings results from p63-dependent alteration of local chromatin

485 structure or chromatin modification by HDACs which may not be directly measured using  
486 plasmid-based MPRA style assays. The full scope of p63-mediated repression, and the extent  
487 of its regulation by DNA sequence alone, might not be observable in a single terminally-  
488 differentiated cell line using only MPRA tools.

489  
490 The relationship between sequence identity and transcriptional output for p63-bound elements  
491 is also complicated by context-dependent activity of other transcription factors binding the same  
492 p63RE motif. The strongest predictor of regulatory element-driven transcriptional output from  
493 our results is the presence of p63RE motifs capable of binding the p63 paralog p53 (Fig. 2D).  
494 These elements are highly active and dependent on the central p53/p63 response element,  
495 which was recently identified as the strongest predictor of regulatory element-driven  
496 transcription (Sahu et al., 2022). The relative activity was preserved in the absence of p53  
497 suggesting that p63 can also drive high-level transcriptional activation (Fig. 2I)(Fig. 4A). How,  
498 though, these motifs drive higher expression by p63 is still unclear. Motif identity is linked to  
499 higher enrichment and transcriptional output by p53 (Fig. 3C,D), but we did not observe any  
500 such relationship for p63. Sites with higher p63 enrichment are not necessarily more active, as  
501 has been observed directly for p53 (Trauernicht et al., 2023). Rather, our data suggest that  
502 ubiquity of p63 binding across cell types better reflects increased transcriptional activity (Fig.  
503 2B). Other features, like increasing local H3K27ac (Kouwenhoven et al., 2015; Qu et al., 2018)  
504 and transcription factor motifs flanking p63REs, including those for traditional transcriptional  
505 activators, contribute to p63-dependent trans-activation (Yang et al., 2006; McDade et al., 2012;  
506 Sethi et al., 2017). Craniofacial development requires specific and combinatorial activity of p63  
507 and other transcription factors at an enhancer for *IRF6* (Rahimov et al., 2008; Fakhouri et al.,  
508 2012, 2014). Our results on p63RE affinity and occupancy are consistent with a model that  
509 enhancers often contain suboptimal binding sites and use motif grammar and syntax to drive  
510 appropriate developmental and stimulus-dependent behaviors (Crocker et al., 2015; Farley et  
511 al., 2015, 2016; Lim et al., 2024).

512  
513 p53 is generally regarded as a universal activator of transcription, whereas p63 either activates  
514 or represses in a context-dependent manner (Fig. 6A) (Fischer et al., 2014). Our data provide  
515 insight into how sequence context, including various sub-classes of the core p63RE motif and  
516 flanking transcription factor motifs, can affect these p63-dependent functions. The mechanisms  
517 controlling this switch between activities, including when p63 serves as a pioneer or  
518 bookmarking factor (Bao et al., 2015; Kouwenhoven et al., 2015), are not fully understood. p63  
519 is also a *bona fide* pioneer transcription factor and controls accessibility at epithelial-specific  
520 regulatory elements (Kouwenhoven et al., 2015; Pattison et al., 2018; Qu et al., 2018; Karsli  
521 Uzunbas et al., 2019; Li et al., 2019; Lin-Shiao et al., 2019; Santos-Pereira et al., 2019; Yu et  
522 al., 2021). Massively parallel reporter assays are powerful tools to study transcriptional  
523 activation and repression, but their design can limit the range of transcription factor activities  
524 that can be directly measured (Inoue and Ahituv, 2015; Trauernicht et al., 2020). Most elements  
525 display p63 expression-dependent chromatin accessibility in epithelial cell types (Fig. 1F) but do  
526 not rely on  $\Delta Np63\alpha$  for their observed transcriptional activity (Fig. 4A). Roles for p63 in  
527 enhancer:promoter interactions, such as those observed during p63-dependent directed  
528 keratinocyte differentiation (Pattison et al., 2018; Li et al., 2019; Qu et al., 2019), would be

529 difficult to measure in a non-genomic context. One other possibility to be investigated in future  
530 studies is that many elements require p63 for *in vivo* chromatin accessibility but not for direct  
531 transcriptional activation or repression. Complementary approaches, like genome-scale MPRA  
532 and loci-specific genetic dissection, are likely required to fully unravel the range of p63-  
533 dependent activities at regulatory elements.

534  
535 The seeming lack of p63-dependent transcriptional control at a substantial number of p63-  
536 bound regulatory elements led us to ask whether cell context might drive differential p63  
537 activities. Enhancers are well-known to exhibit cell type and context-dependent activities  
538 controlled by variable expression of transcription factors and co-factors (Spitz and Furlong,  
539 2012; Heinz et al., 2015). p63 expression is strongly lineage restricted during development and  
540 homeostasis and varied p63 levels have been linked to human cancers (Massion et al., 2003;  
541 Graziano and De Laurenzi, 2011; Tucci et al., 2012; Pickering et al., 2014; Saladi et al., 2017).  
542 Elevated p63 expression is strongly linked to pro-survival pathways in squamous cell  
543 carcinomas (SCC) (Thurfjell et al., 2005; Ramsey et al., 2013; Abraham et al., 2018). These  
544 collective observations led us to investigate whether p63-dependent regulatory element  
545 behavior varied across epithelial cell contexts. SCC-25, a head and neck squamous cell  
546 carcinoma cell line, in particular showed varied activity of p63-dependent regulatory elements  
547 (Fig. 5B,C). Although more elements displayed p63-dependent repression than in MCF-10A,  
548 these elements lacked specific enrichment for transcription factor motifs that might cooperate  
549 with p63 to reduce transcriptional output (Table S3). In contrast, p63-dependent activation in  
550 SCC-25 was coupled with enrichment of different TF motifs than those associated with  
551 activation in MCF10A including a range of factors with known epithelial functions, like the Maf  
552 and Forkhead families (Fig. 5E) (Lopez-Pajares et al., 2015; Napoli et al., 2024). Regulatory  
553 elements with cell-specific activities appear to utilize different combinations of co-enriching  
554 motifs alongside p63 (Donohue et al., 2022). The extent to which p63 amplification or other  
555 transcription factor availability drives differential p63-dependent activities at gene regulatory  
556 elements, both during development and disease, requires more investigation to unravel. This  
557 might include combining advances in genome-scale reporter assays, single-cell spatial  
558 transcriptomics, and machine-learning assisted design that have led to the ability to design  
559 synthetic enhancers with defined cell type-specific activities (Taskiran et al., 2024).

560  
561 Transcription factors are commonly spliced to produce various isoforms which often display  
562 differential activities (Wang et al., 2008; Lambourne et al., 2024). The role of p63 at regulatory  
563 elements is further complicated by the complexities of transcription factor isoforms and  
564 paralogs. The constitutively active TAp63 $\beta$  isoform activated transcription at most regulatory  
565 elements (Fig. 5H) similar to near-universal activation by p53 (Verfaillie et al., 2016; Peng et al.,  
566 2020; Sahu et al., 2022). TAp63 $\alpha$  is critical in the germline and in late keratinocyte differentiation  
567 and TAp63 $\alpha$  has stimulus-dependent activity unlike  $\Delta$ Np63 isoforms (Koster et al., 2004; Truong  
568 et al., 2006; Beyer et al., 2011; Deutsch et al., 2011). Gene regulatory elements activated  
569 uniquely by TAp63 isoforms are bound by both TA and  $\Delta$ Np63 isoforms. The role of  $\Delta$ N  
570 isoforms at these elements then may be to establish and bookmark local chromatin structure for  
571 later TA isoform activity, as  $\Delta$ Np63 can do for regulated cell lineage-specific p53 activity (Karsli  
572 Uzunbas et al., 2019). The interplay between transcription factor paralogs with overlapping

573 DNA binding activity can drive variable gene regulatory element activity (Fig. 6B). p53 and p73  
574 share considerable tissue expression and binding site overlap with p63 (Marshall et al., 2021),  
575 so the extent to which paralog expression influences p63-dependent behaviors should not be  
576 overlooked. Similarly, p73 may also influence p63 activity through formation of mixed p63:p73  
577 heterotetramers suggesting yet another mechanism influencing regulatory element behavior  
578 (Strubel et al., 2023). Our results suggest that significant additional effort should be placed into  
579 identifying how cell type, developmental stage, or stimulus-dependent conditions might lead to  
580 p63 isoform switching, paralog expression, and, ultimately, varied p63-dependent gene  
581 regulatory activity (Fig. 6B).

582  
583 In conclusion, we present a near genome-scale analysis of p63-dependent regulatory element  
584 activity. Our data are consistent with varying roles of p63 in literature and suggest that while  
585 sequence content is important, other local cofactors, isoform switching, paralog expression, and  
586 chromatin are critical context-dependent regulators of p63-dependent CRE activity.  
587 Unraveling the full scope of p63 activities will likely require multiple complementary approaches  
588 including specific assays focused on p63-dependent chromatin remodeling, native approaches  
589 for examining sequence content such as genome editing, and new computational tools like AI  
590 and deep learning.

591

## 592 **MATERIALS AND METHODS**

593

### 594 *Cell culture*

595 All human mammary epithelial cell lines MCF-10A TP53<sup>+/+</sup> and TP53<sup>-/-</sup> (Sigma-Millipore  
596 clls1049) were cultured in 1:1 Dulbecco's Modified Eagle's Medium: Ham's F-12 (Gibco,  
597 #11330-032), supplemented with 5% Horse Serum, (Gibco, #16050-122), 20 ng/mL epidermal  
598 growth factor (Peprotech, #AF-100-15), 0.5 µg/mL hydrocortisone (Sigma, #H-0888), 100 ng/mL  
599 cholera toxin (Sigma, #C-8052), 10 µg/mL insulin (Sigma, #I-1882), and 1% penicillin-  
600 streptomycin (Gibco, #15240-062). MCF10A TP53<sup>-/-</sup> cells were obtained from Sigma-Millipore  
601 (clls1049) and were cultured Human HNSCC cell line SCC-25 (kind gift of C. Michael DiPersio,  
602 Albany Medical College) were cultured in 1:1 Dulbecco's Modified Eagle's Medium: Ham's F-12,  
603 supplemented with 10% FBS (Corning, #35-016-CV), 1% penicillin-streptomycin and 400 ng/ml  
604 hydrocortisone. Human transformed keratinocyte cell line HaCat and HEK293FT cells were  
605 cultured in Dulbecco's Modified Eagle's Medium 1X (Corning 10-013-CV) and supplemented  
606 with 10% FBS and 1% penicillin-streptomycin. All cell lines were cultured at 37°C and 5% CO<sub>2</sub>.

607

### 608 *Lentiviral Production*

609 Lentiviral particles were packaged by transfecting 600ng psPAX2, 400ng of pMD2.G,  
610 and 1µg of pCW57.1 containing either TAp63β or β-glucuronidase (GUS) control in HEK293FT  
611 cells at a density of 600,000 per well. pCW57.1 (pCW57.1 was a gift from David Root, Addgene  
612 plasmid # 41393 ; <http://n2t.net/addgene:41393> ; RRID:Addgene\_41393), psPAX2, and  
613 pMD2.G (psPAX2 and pMD2.G were a gift from Didier Trono, Addgene plasmid # 12260 ;  
614 <http://n2t.net/addgene:12260> ; RRID:Addgene\_12260) were obtained from Addgene. GUS  
615 control plasmid was provided as part of the LR Clonase II enzyme kit (Invitrogen 11791020).  
616 Lentiviral supernatants were collected at 24 and 48 hours and concentrated via spin dialysis.

617 Viral supernatants were added to MCF-10A cells with 8ug/ml polybrene for 24 hours and then  
618 replaced with fresh media. 2ug/ml puromycin was added 48 hours after infection and cells were  
619 selected for 72 hours.

#### 620 621 *Western blotting*

622 Protein was isolated using custom made RIPA buffer (50 mM Tris-HCl pH 7.4, 150 mM  
623 NaCl, 1% NP-40, 0.5% sodium deoxycholate, 0.1% SDS, 1mM EDTA, 1% Triton x-100)  
624 supplemented with protease inhibitor (Pierce, 78442). Concentration of isolated protein was  
625 measured using a microBCA kit (Pierce, 23227) and 25µg was loaded on a 4-12% Bis-Tris  
626 protein gel (Invitrogen, NP0321BOX). Protein size was analyzed using PageRuler™ Prestained  
627 Protein Ladder (Thermo 26616). Membranes were blocked in 5% non-fat milk in TBS-T.  
628 Antibodies used included rabbit anti-ΔNp63 antibody (Cell Signaling E6Q3O), mouse anti-p53  
629 (BD Biosciences 554293), mouse anti-TAp63 (BioLegend 938102) rabbit anti-GAPDH antibody  
630 (Cell Signaling D16H11), and rabbit anti-β-Glucuronidase (Sigma Aldrich G5545).

#### 631 632 *Massively parallel reporter assay (MPRA) design*

633 MPRA query regions were selected from a recent analysis of multiple p63 ChIP-seq  
634 datasets (Riege et al., 2020). Only p63 binding events observed in 8 or more independent  
635 experiments and containing p63 response element (p63RE) sequences (17,310 locations) were  
636 considered for analysis due to DNA synthesis constraints. MPRA regions were centered on the  
637 p63RE and were extended to a total length of 119 or 120 bp based on the length of the p63RE.  
638 Genomic coordinates corresponding to each p63 MPRA region were used to extract DNA  
639 sequence information from the hg38 UCSC genome assembly using bedtools. Either the entire  
640 MPRA sequence (full shuffle), the p63RE (shuffle), or the regions flanking the p63RE (flank  
641 shuffle) were randomly scrambled, while preserving GC content, to produce three variants.  
642 Position weight matrices for the p63RE were generated using consensusMatrix (Biostrings R  
643 package) and visualized using seqLogo. A fourth variant (mutant) was designed where  
644 consensus nucleotides found within the p63RE at a frequency greater than 75% were  
645 substituted to preserve GC content. A schematic of all substitutions can be found in Figure 1A.  
646 Adapter sequences were then added to the 5' (5'-TCCCTACACGACGCTCTCCGATCT) and 3'  
647 (5'-AGATCGGAAGAGCACACGTCTGAAC) end of each MPRA sequence. Sequences for all  
648 MPRA regions can be found in Table S1. An oligo pool containing all 86,550 reporter sequences  
649 was synthesized by GenScript (Piscataway, NJ, USA).

#### 650 651 *Cloning oligo pool library*

652 MPRA oligo plasmid pool was cloned as described with the following adjustments  
653 (Neumayr et al., 2022). Plasmid backbone pGB118, with added Illumina i5/i7 sequences  
654 flanking the cloning site, was digested with *AgeI* and *Sall* as described (Baniulyte et al., 2023).  
655 pGB118 was based on hSTARR-seq\_ORI vector, which was a gift from Alexander Stark  
656 (Addgene plasmid # 99296 ; <http://n2t.net/addgene:99296> ; RRID:Addgene\_99296). The oligo  
657 pool was amplified using Q5 polymerase and SL1947 (5'-TCCCTACACGACGCTCTTC) and  
658 SL1948 (5'-GTTTCAGACGTGTGCTCTTC) primers for 15 cycles. Amplicons were then cloned  
659 into pGB118 using HiFi assembly (NEB M0492S) and HiFi reactions were transformed into

660 DH5alpha cells (NEB C2987H) and grown in LB culture. Plasmid library was purified using  
661 ZymoPURE Gigaprep kit (Zymo D4204).

662

### 663 *Plasmid pool transfection, library preparation and sequencing*

664 Two biological replicates were performed for each cell type and condition at  
665 approximately 50 million cells per replicate and one biological replicate was performed for  
666 isoform (GUS, TAp63 $\beta$ ) overexpression assay. 10  $\mu$ g of plasmid library were transfected per 5  
667 million cells via lipofection (Polyplus #101000046, #101000025). For TAp63 $\beta$  inducible cell line  
668 and negative control (GUS) cell line, doxycycline was added at 500 ng/ml at the same time as  
669 transfection. Cells were harvested after 24 hours and total RNA was extracted (Quick RNA,  
670 Zymo, #R1055). 30  $\mu$ g per replicate of poly-adenylated mRNA was isolated using oligo d(T)  
671 beads (NEB E7490L). Resulting mRNA was split into 6 separate reactions and cDNA was  
672 synthesized using a gene-specific primer (5'-CTCATCAATGTATCTTATCATGTCTG-3') and  
673 MultiScribe Reverse Transcriptase (Invitrogen, 4311235). Following cDNA synthesis, all cDNA  
674 samples were pooled and one Junction-PCR reaction was performed with 16 cycles (5'-  
675 TCGTGAGGCACTGGGCAGGTGTC,CTTATCATGTCTGCTCGAAGC-3') and i5 and i7 primers  
676 from NEBNext Oligo Kit (E7600S) were used for Illumina barcoding with between 5 and 9  
677 cycles. MPRA plasmid DNA pools were amplified with i5 and i7 primers as a control for oligo  
678 representation. All libraries were pooled and sequenced as single-end, 100bp on an Illumina  
679 NextSeq 2000 instrument at the University at Albany Center for Functional Genomics.

680

### 681 *MPRA library data analysis*

682 FASTQ files for plasmid DNA and enhancer RNA libraries were mapped using exact  
683 pattern match using custom Python scripts. Enhancers that had less than 5 reads were  
684 removed. Raw read count table is available under Gene Expression Omnibus accession  
685 number GSE266670. Additionally, for Figures 1-4 were MCF-10A and MCF-10A *TP53*<sup>-/-</sup> cell  
686 lines were used, only enhancers that had a match for every enhancer variant (WT, mut, shuffle,  
687 flankShuffle, fullShuffle) were kept (n = 13,696). Where MCF-10A *TP53*<sup>-/-</sup>, HaCaT and SCC-25  
688 (Fig. 5 B-E) or MCF-10A TAp63 $\beta$  and GUS overexpression cell lines were considered,  
689 enhancers that only had a WT and mut matched variants were kept (N = 8,566 and N = 16,143,  
690 respectively). All reads were normalized to the total number of reads per sample and expression  
691 values are represented as RNA/DNA ratio and averaged between the replicates. Normalized  
692 expression values and enhancers considered for each figure are listed in Table S2. Statistical  
693 tests were performed using Python packages (SciPy, scikit-posthocs).

694

### 695 *Data Integration*

696 MCF-10A p63, p53, H3K27ac, H3K4me2, and H3K4me3 datasets were downloaded  
697 from Gene Expression Omnibus accession GSE111009 (Karsli Uzunbas et al., 2019). Raw data  
698 were mapped to the GRCh38 reference assembly using hisat2 and biological replicates were  
699 combined using the merge function of samtools (Li et al., 2009; Kim et al., 2019). Enrichment at  
700 MPRA regions was quantified and visualized using deepTools (Ramírez et al., 2016). p53 and  
701 p63 enrichment data were quantified within 1bp bins across the entire p53/p63RE motif location  
702 and heatmaps were generated using 10bp bins across a region spanning +/- 1,000 bp from the  
703 p53/p63RE motif. Datasets used to integrate ENCODE ChromHMM, candidate Cis Regulatory

704 Elements (cCRE), and DNase Hypersensitivity Clusters (DHS) with MPRA genomic locations  
705 were obtained from repositories as specified in Table S4. Intersections between p63 CRE  
706 regions and various datasets were performed using either bedTools or BigBedtoBed (Kent et  
707 al., 2010; Quinlan and Hall, 2010). Motif enrichment analyses were performed using HOMER  
708 (Heinz et al., 2010; Duttke et al., 2019). GC and dinucleotide content analyses were performed  
709 using custom nucleotide counting scripts in Python.

710

#### 711 *Data availability*

712 MPRA datasets from this manuscript are available under Gene Expression Omnibus  
713 (GEO) accession GSE266670.

714

#### 715 **Acknowledgments**

716

717 This work was supported by NIH R35 GM138120 to MAS. DLW was partially supported by NIH  
718 T32 GM132066. The authors would like to thank the University at Albany Center for Functional  
719 Genomics for sequencing support and the RNA Institute at the University at Albany for  
720 additional equipment support and for generous support of the trainees on this manuscript.

## 721 Figure Legends

722

723 **Figure 1.** (A) STARR-Seq MPRA design. A p63 response element (RE) binding motif was  
724 centered within each putative cis-regulatory element (CRE) with a total length of up to 120  
725 nucleotides. See Material and Methods and Table S1 for more information. Each wild-type (WT)  
726 element has a variant with p63RE mutation (mut or shuffle), scrambled flanking region  
727 (flankShuffle) or fully scrambled variant (fullShuffle). All elements preserve total GC content. (B)  
728 Position Weight Matrix (PWM) of the canonical WT p63RE or a mutant generated in this study  
729 (mut). (C) Distribution of CREs used in this study based on distance to the nearest RefSeq TSS.  
730 (D) Fraction of CREs found in intergenic or intragenic regions. (E) Distribution of CREs within  
731 ENCODE cCRE annotated functional elements. (F) Fraction of CREs occurring within DNase  
732 Hypersensitive (DHS) clusters, denoted as “open”. (G) Predicted regulatory status of CREs  
733 based on chromHMM chromatin state modeling. (I) Heatmaps representing p63, H3K27ac,  
734 H3K4me2 and H3K4me3 enrichment in MCF-10A cells at CRE locations used in this study. (J)  
735 Activity of CRE variants in MCF-10A cell line shown as a ratio of sequenced STARR-seq RNA  
736 reads to the original DNA library. *p*-values were calculated using Kruskal-Wallis test followed by  
737 Dunn’s *post-hoc* test and Bonferroni adjustment (\*\*\*\**p*-value < 0.0001).

738

739 **Figure 2.** Box-plot showing relationship between meta-analysis-based p63 binding observation  
740 score and p63 ChIP-seq enrichment in the MCF-10A cell line (A) or WT CRE activity from the  
741 STARR-seq assay (B). (C) Correlation between WT or mut CRE activity and p63 ChIP-seq  
742 enrichment in MCF-10A cells (Spearman’s  $\rho=0.127$ ,  $p=2.26e-48$  for WT comparison and  $\rho=-0.0$ ,  
743  $p=0.98$  for mut). (D) WT and mut CRE activity for Unique p63RE or p53RE+p63RE motif types  
744 with number of each motif type indicated on the *x*-axis (\*\*\*\*: *p*-value < 0.0001, *Wilcoxon* signed-  
745 rank test) (E) Box-plot showing relationship between meta-analysis-based p53 observation  
746 score and p53 ChIP-seq enrichment in MCF-10A cell line. (F) Correlation between WT or mut  
747 activity and p53 ChIP-seq enrichment in MCF-10A cells (Spearman’s  $\rho=0.405$ ,  $p=0.0$  for WT  
748 comparison and  $\rho=-0.094$ ,  $p=4.4e-27$  for mut). (G) Western blot analysis of p53 and  $\Delta$ Np63  
749 expression in MCF-10A and MCF-10A TP53<sup>-/-</sup> cells. GAPDH is used as a loading control. (H)  
750 p53RE+p63RE enhancer activity in WT or TP53<sup>-/-</sup> MCF-10A cell lines (\*\*\*\*: *p*-value < 0.0001,  
751 *Wilcoxon* signed-rank test). (I) Differences in WT CRE activity between p63RE motif types in  
752 MCF-10A TP53<sup>-/-</sup> cells.

753

754 **Figure 3.** Analysis of p63RE motif class and CRE activity. (A) PWM of p53RE+p63RE motif  
755 classes, with stars indicating nucleotide substitutions in mut variants. p63 (B) or p53 (C) ChIP-  
756 seq enrichment in MCF-10A cells within each p53RE+p63RE motif class. (D) WT or mut  
757 enhancer activity in MCF-10A (D) or MCF-10A TP53<sup>-/-</sup> (E) within each p53RE+p63RE motif  
758 class. (F) PWM of Unique p63RE motif classes, with stars indicating nucleotide substitutions in  
759 mut variants. (G) p63 ChIP-seq enrichment in MCF-10A cells within each Unique p63RE motif  
760 class. WT or mut enhancer activity in MCF-10A (H) or MCF-10A TP53<sup>-/-</sup> (I) based on Unique  
761 p63RE motif class. (J) Dinucleotide repeat motif frequency in CREs. (K) Average GC content  
762 across CRE regions separated by motif type. GC content was determined using a 10 nt sliding  
763 window approach. Shaded area represents a 95% confidence interval. (L) Average CRE GC  
764 content of Unique p63RE (L) or p53RE+p63RE (M) within each motif class. Statistical

765 comparisons were computed using either Mann-Whitney U test (B, C, G, L, M) or Wilcoxon  
766 signed-rank test (D, E, H, I).  $p$ -values are indicated as *ns*:  $0.05 < p$ , \*\*:  $0.001 < p \leq 0.01$ , \*\*\*:  
767  $0.0001 < p \leq 0.001$ , \*\*\*\*:  $p \leq 0.0001$ .

768  
769 **Figure 4.** Functional characterization of p63-dependent CRE transcriptional activity. Functional  
770 activity is defined by 1.5 fold-change (WT/mut) cutoff where “Activating” is  $>1.5$ , “Repressing” is  
771  $<1.5$  and the remaining are defined as “Unchanged”. (A) Distribution of enhancer function in  
772 MCF-10A TP53<sup>-/-</sup> cells in each motif type. Distribution of enhancer function in p53RE+p63RE  
773 (B) motif classes or p63 UniqueRE (C) motif classes as defined in Fig. 3A, F. (D) Average GC  
774 content across enhancer region by enhancer function. Shaded area represents a 95%  
775 confidence interval. (E) WT, mut and flankShuffle enhancer activity in MCF-10A TP53<sup>-/-</sup> cells by  
776 function (\*\*\*\*:  $p$ -value  $< 0.0001$ , Wilcoxon signed-rank test). (F) Top 30 enriched motifs in  
777 “Activating” or “Repressing” enhancer groups relative to “Unchanged” enhancer groups. Motif  
778 enrichment was performed using HOMER (Heinz et al., 2010; Duttke et al., 2019). Dot size  
779 represents the fraction of CREs containing the specified motif. Color scale indicates Bonferroni-  
780 corrected  $p$ -value.

781  
782 **Figure 5.** Cell type and context-dependent effect on p63-dependent CRE activity. (A) Western  
783 blot analysis of p63 expression in MCF-10A TP53<sup>-/-</sup>, HaCaT and SCC-25 cells. GAPDH is used  
784 as a loading control. (B) Distribution of p63-dependent CRE function in MCF-10A TP53<sup>-/-</sup>,  
785 HaCat, or SCC-25 cells (N=8,566). (C) Sankey diagram derived from (B) depicting changes in  
786 p63-dependent CRE function across three cell types. Numbers indicate CRE counts in each  
787 group and cell line. (D-E) Scatter plots highlighting transcription factor motifs enriched in p63-  
788 activated CREs that are shared (D) between SCC-25 and MCF-10A TP53<sup>-/-</sup> cell lines or  
789 uniquely enriched in each (E). Dot size represents fold-change enrichment over background.  
790 Color scale indicates log-transformed  $p$ -value. (F) Western blot showing Doxycycline-inducible  
791 TAp63 $\beta$  or GUS control expression in MCF-10A cells. Cells were treated for 8h with either 500  
792 ng/ml Dox or water as vehicle control. (G) WT and mut CRE activity (N=16,143) in either control  
793 (GUS) or TAp63 $\beta$  induced cell line (\*\*\*\*:  $p$ -value  $< 0.0001$ , Wilcoxon signed-rank test). (H)  
794 Distribution of p63-dependent CRE function in either control or TAp63 $\beta$  induced cell line.

795  
796 **Figure 6.** (A) Schematic illustrating differential activity of  $\Delta$ Np63 $\alpha$  at *cis*-regulatory elements.  
797 While sequences can elicit either  $\Delta$ Np63 $\alpha$ -dependent transcriptional activation or repression,  
798 many appear  $\Delta$ Np63 $\alpha$ -independent. (B) Schematic depicting how p63 paralogs and isoforms  
799 binding to the same element can elicit different outcomes compared to  $\Delta$ Np63 $\alpha$ , including high  
800 level transcriptional activation by p53 and TAp63. Other p63 paralogs and isoforms may have  
801 different activities depending on the presence of particular protein domains, and are not  
802 depicted here.  $\Delta$ Np63 $\alpha$  activity at *cis*-regulatory elements also can change based on cell context  
803 or on the availability of local transcription factors, although the molecular grammar of these  
804 interactions and how they give rise to differential function remain unclear.

805  
806 **Table S1.** Relevant CRE information and sequences used in this study.

807

808 **Table S2.** Normalized expression values (RNA/DNA) for cell type- and CRE variant-matched  
809 enhancers used in this study.

810

811 **Table S3.** HOMER knownResults output for “Activating” or “Repressing” CREs in MCF-10A  
812 *TP53*<sup>-/-</sup> and SCC-25 cell lines.

813

814 **Table S4.** Data sources.

## 815 Bibliography

- 816
- 817 Abraham, C. G., Ludwig, M. P., Andrysiak, Z., Pandey, A., Joshi, M., Galbraith, M. D., et al.  
818 (2018).  $\Delta$ Np63 $\alpha$  Suppresses TGFB2 Expression and RHOA Activity to Drive Cell  
819 Proliferation in Squamous Cell Carcinomas. *Cell Reports* 24, 3224–3236. doi:  
820 10.1016/j.celrep.2018.08.058
- 821 Amiel, J., Bougeard, G., Francannet, C., Raclin, V., Munnich, A., Lyonnet, S., et al. (2001).  
822 TP63 gene mutation in ADULT syndrome. *Eur J Hum Genet* 9, 642–645. doi:  
823 10.1038/sj.ejhg.5200676
- 824 Arnold, C. D., Gerlach, D., Stelzer, C., Boryn, L. M., Rath, M., and Stark, A. (2013). Genome-  
825 wide quantitative enhancer activity maps identified by STARR-seq. *Science* 339, 1074–  
826 7. doi: 10.1126/science.1232542
- 827 Bamford, S., Dawson, E., Forbes, S., Clements, J., Pettett, R., Dogan, A., et al. (2004). The  
828 COSMIC (Catalogue of Somatic Mutations in Cancer) database and website. *Br J*  
829 *Cancer* 91, 355–358. doi: 10.1038/sj.bjc.6601894
- 830 Baniulyte, G., Durham, S. A., Merchant, L. E., and Sammons, M. A. (2023). Shared Gene  
831 Targets of the ATF4 and p53 Transcriptional Networks. *Molecular and Cellular Biology* 0,  
832 1–24. doi: 10.1080/10985549.2023.2229225
- 833 Bao, X., Rubin, A. J., Qu, K., Zhang, J., Giresi, P. G., Chang, H. Y., et al. (2015). A novel ATAC-  
834 seq approach reveals lineage-specific reinforcement of the open chromatin landscape  
835 via cooperation between BAF and p63. *Genome Biology* 16, 284. doi: 10.1186/s13059-  
836 015-0840-9
- 837 Barral, A., and Zaret, K. S. (2023). Pioneer factors: roles and their regulation in development.  
838 *Trends in Genetics* 0. doi: 10.1016/j.tig.2023.10.007
- 839 Beyer, U., Moll-Rocek, J., Moll, U. M., and Dobbstein, M. (2011). Endogenous retrovirus  
840 drives hitherto unknown proapoptotic p63 isoforms in the male germ line of humans and  
841 great apes. *Proc Natl Acad Sci U S A* 108, 3624–3629. doi: 10.1073/pnas.1016201108
- 842 Biddie, S. C., John, S., Sabo, P. J., Thurman, R. E., Johnson, T. A., Schiltz, R. L., et al. (2011).  
843 Transcription factor AP1 potentiates chromatin accessibility and glucocorticoid receptor  
844 binding. *Mol. Cell* 43, 145–155. doi: 10.1016/j.molcel.2011.06.016
- 845 Bougeard, G., Hadj-Rabia, S., Faivre, L., Sarafan-Vasseur, N., and Frébourg, T. (2003). The  
846 Rapp–Hodgkin syndrome results from mutations of the TP63 gene. *Eur J Hum Genet*  
847 11, 700–704. doi: 10.1038/sj.ejhg.5201004
- 848 Candi, E., Rufini, A., Terrinoni, A., Dinsdale, D., Ranalli, M., Paradisi, A., et al. (2006).  
849 Differential roles of p63 isoforms in epidermal development: selective genetic  
850 complementation in p63 null mice. *Cell Death Differ* 13, 1037–1047. doi:  
851 10.1038/sj.cdd.4401926
- 852 Castro-Mondragon, J. A., Riudavets-Puig, R., Rauluseviciute, I., Berhanu Lemma, R., Turchi, L.,  
853 Blanc-Mathieu, R., et al. (2022). JASPAR 2022: the 9th release of the open-access  
854 database of transcription factor binding profiles. *Nucleic Acids Research* 50, D165–  
855 D173. doi: 10.1093/nar/gkab1113
- 856 Celli, J., Duijf, P., Hamel, B. C. J., Bamshad, M., Kramer, B., Smits, A. P. T., et al. (1999).  
857 Heterozygous Germline Mutations in the p53 Homolog p63 Are the Cause of EEC  
858 Syndrome. *Cell* 99, 143–153. doi: 10.1016/S0092-8674(00)81646-3
- 859 Colbran, L. L., Chen, L., and Capra, J. A. (2017). Short DNA sequence patterns accurately  
860 identify broadly active human enhancers. *BMC Genomics* 18, 536. doi: 10.1186/s12864-  
861 017-3934-9
- 862 Coutandin, D., Osterburg, C., Srivastav, R. K., Sumyk, M., Kehroesser, S., Gebel, J., et al.  
863 (2016). Quality control in oocytes by p63 is based on a spring-loaded activation  
864 mechanism on the molecular and cellular level. *eLife* 5, e13909. doi:

- 865 10.7554/eLife.13909
- 866 Crocker, J., Abe, N., Rinaldi, L., McGregor, A. P., Frankel, N., Wang, S., et al. (2015). Low  
867 affinity binding site clusters confer hox specificity and regulatory robustness. *Cell* 160,  
868 191–203. doi: 10.1016/j.cell.2014.11.041
- 869 Currey, L., Thor, S., and Piper, M. (2021). TEAD family transcription factors in development and  
870 disease. *Development* 148, dev196675. doi: 10.1242/dev.196675
- 871 Deutsch, G. B., Zielonka, E. M., Coutandin, D., Weber, T. A., Schäfer, B., Hannewald, J., et al.  
872 (2011). DNA Damage in Oocytes Induces a Switch of the Quality Control Factor TAp63α  
873 from Dimer to Tetramer. *Cell* 144, 566–576. doi: 10.1016/j.cell.2011.01.013
- 874 Donohue, L. K. H., Guo, M. G., Zhao, Y., Jung, N., Bussat, R. T., Kim, D. S., et al. (2022). A cis-  
875 regulatory lexicon of DNA motif combinations mediating cell-type-specific gene  
876 regulation. *Cell Genom* 2, 100191. doi: 10.1016/j.xgen.2022.100191
- 877 Duttke, S. H., Chang, M. W., Heinz, S., and Benner, C. (2019). Identification and dynamic  
878 quantification of regulatory elements using total RNA. *Genome Res.* doi:  
879 10.1101/gr.253492.119
- 880 el-Deiry, W. S., Kern, S. E., Pietenpol, J. A., Kinzler, K. W., and Vogelstein, B. (1992). Definition  
881 of a consensus binding site for p53. *Nat Genet* 1, 45–49. doi: 10.1038/ng0492-45
- 882 Ernst, J., and Kellis, M. (2015). Large-scale imputation of epigenomic datasets for systematic  
883 annotation of diverse human tissues. *Nat. Biotechnol.* 33, 364–376. doi:  
884 10.1038/nbt.3157
- 885 Fakhouri, W. D., Rahimov, F., Attanasio, C., Kouwenhoven, E. N., Ferreira De Lima, R. L., Felix,  
886 T. M., et al. (2014). An etiologic regulatory mutation in IRF6 with loss- and gain-of-  
887 function effects. *Hum Mol Genet* 23, 2711–20. doi: 10.1093/hmg/ddt664
- 888 Fakhouri, W. D., Rhea, L., Du, T., Sweezer, E., Morrison, H., Fitzpatrick, D., et al. (2012).  
889 MCS9.7 enhancer activity is highly, but not completely, associated with expression of  
890 Irf6 and p63. *Dev Dyn* 241, 340–349. doi: 10.1002/dvdy.22786
- 891 Farley, E. K., Olson, K. M., Zhang, W., Brandt, A. J., Rokhsar, D. S., and Levine, M. S. (2015).  
892 Suboptimization of developmental enhancers. *Science* 350, 325–328. doi:  
893 10.1126/science.aac6948
- 894 Farley, E. K., Olson, K. M., Zhang, W., Rokhsar, D. S., and Levine, M. S. (2016). Syntax  
895 compensates for poor binding sites to encode tissue specificity of developmental  
896 enhancers. *Proc Natl Acad Sci U S A* 113, 6508–6513. doi: 10.1073/pnas.1605085113
- 897 Fischer, M., Steiner, L., and Engeland, K. (2014). The transcription factor p53: not a repressor,  
898 solely an activator. *Cell Cycle* 13, 3037–3058. doi: 10.4161/15384101.2014.949083
- 899 Fisher, M. L., Balinth, S., and Mills, A. A. (2020). p63-related signaling at a glance. *J Cell Sci*  
900 133. doi: 10.1242/jcs.228015
- 901 Fletcher, R. B., Prasol, M. S., Estrada, J., Baudhuin, A., Vranizan, K., Choi, Y. G., et al. (2011).  
902 p63 Regulates Olfactory Stem Cell Self-Renewal and Differentiation. *Neuron* 72, 748–  
903 759. doi: 10.1016/j.neuron.2011.09.009
- 904 Gebel, J., Tuppi, M., Krauskopf, K., Coutandin, D., Pitzius, S., Kehrloesser, S., et al. (2017).  
905 Control mechanisms in germ cells mediated by p53 family proteins. *Journal of Cell*  
906 *Science* 130, 2663–2671. doi: 10.1242/jcs.204859
- 907 Graziano, V., and De Laurenzi, V. (2011). Role of p63 in cancer development. *Biochimica et*  
908 *Biophysica Acta (BBA) - Reviews on Cancer* 1816, 57–66. doi:  
909 10.1016/j.bbcan.2011.04.002
- 910 Hager, G. L., McNally, J. G., and Misteli, T. (2009). Transcription Dynamics. *Molecular Cell* 35,  
911 741–753. doi: 10.1016/j.molcel.2009.09.005
- 912 Halfon, M. S. (2020). Silencers, Enhancers, and the Multifunctional Regulatory Genome. *Trends*  
913 *in Genetics* 36, 149–151. doi: 10.1016/j.tig.2019.12.005
- 914 Heinz, S., Benner, C., Spann, N., Bertolino, E., Lin, Y. C., Laslo, P., et al. (2010). Simple  
915 combinations of lineage-determining transcription factors prime cis-regulatory elements

- 916 required for macrophage and B cell identities. *Mol. Cell* 38, 576–589. doi:  
917 10.1016/j.molcel.2010.05.004
- 918 Heinz, S., Romanoski, C. E., Benner, C., and Glass, C. K. (2015). The selection and function of  
919 cell type-specific enhancers. *Nature Reviews Molecular Cell Biology* 16, 144–154. doi:  
920 10.1038/nrm3949
- 921 Inoue, F., and Ahituv, N. (2015). Decoding enhancers using massively parallel reporter assays.  
922 *Genomics* 106, 159–164. doi: 10.1016/j.ygeno.2015.06.005
- 923 Janky, R., Verfaillie, A., Imrichová, H., Van de Sande, B., Standaert, L., Christiaens, V., et al.  
924 (2014). iRegulon: From a Gene List to a Gene Regulatory Network Using Large Motif  
925 and Track Collections. *PLoS Computational Biology* 10, e1003731. doi:  
926 10.1371/journal.pcbi.1003731
- 927 Jindal, G. A., and Farley, E. K. (2021). Enhancer grammar in development, evolution, and  
928 disease: dependencies and interplay. *Developmental Cell* 56, 575–587. doi:  
929 10.1016/j.devcel.2021.02.016
- 930 Kalluri, R., and Weinberg, R. A. (2009). The basics of epithelial-mesenchymal transition. *J Clin*  
931 *Invest* 119, 1420–1428. doi: 10.1172/JCI39104
- 932 Karsli Uzunbas, G., Ahmed, F., and Sammons, M. A. (2019). Control of p53-dependent  
933 transcription and enhancer activity by the p53 family member p63. *J. Biol. Chem.* doi:  
934 10.1074/jbc.RA119.007965
- 935 Katoh, I., Maehata, Y., Moriishi, K., Hata, R.-I., and Kurata, S. (2019). C-terminal  $\alpha$  Domain of  
936 p63 Binds to p300 to Coactivate  $\beta$ -Catenin. *Neoplasia* 21, 494–503. doi:  
937 10.1016/j.neo.2019.03.010
- 938 Kent, W. J., Zweig, A. S., Barber, G., Hinrichs, A. S., and Karolchik, D. (2010). BigWig and  
939 BigBed: enabling browsing of large distributed datasets. *Bioinformatics* 26, 2204–2207.  
940 doi: 10.1093/bioinformatics/btq351
- 941 Kim, D., Paggi, J. M., Park, C., Bennett, C., and Salzberg, S. L. (2019). Graph-based genome  
942 alignment and genotyping with HISAT2 and HISAT-genotype. *Nat Biotechnol* 37, 907–  
943 915. doi: 10.1038/s41587-019-0201-4
- 944 Klein, K., Habiger, C., Iftner, T., and Stubenrauch, F. (2020). A TGF- $\beta$ - and p63-Responsive  
945 Enhancer Regulates IFN- $\kappa$  Expression in Human Keratinocytes. *The Journal of*  
946 *Immunology*. doi: 10.4049/jimmunol.1901178
- 947 Koster, M. I., Kim, S., Mills, A. A., DeMayo, F. J., and Roop, D. R. (2004). p63 is the molecular  
948 switch for initiation of an epithelial stratification program. *Genes Dev.* 18, 126–131. doi:  
949 10.1101/gad.1165104
- 950 Kouwenhoven, E. N., Oti, M., Niehues, H., van Heeringen, S. J., Schalkwijk, J., Stunnenberg, H.  
951 G., et al. (2015). Transcription factor p63 bookmarks and regulates dynamic enhancers  
952 during epidermal differentiation. *EMBO reports* 16, 863–878. doi:  
953 10.15252/embr.201439941
- 954 Krauskopf, K., Gebel, J., Kazemi, S., Tuppi, M., Löhr, F., Schäfer, B., et al. (2018). Regulation of  
955 the Activity in the p53 Family Depends on the Organization of the Transactivation  
956 Domain. *Structure* 26, 1091-1100.e4. doi: 10.1016/j.str.2018.05.013
- 957 Kulkarni, M. M., and Arnosti, D. N. (2003). Information display by transcriptional enhancers.  
958 *Development* 130, 6569–6575. doi: 10.1242/dev.00890
- 959 Lambert, S. A., Jolma, A., Campitelli, L. F., Das, P. K., Yin, Y., Albu, M., et al. (2018). The  
960 Human Transcription Factors. *Cell* 172, 650–665. doi: 10.1016/j.cell.2018.01.029
- 961 Lambourne, L., Mattioli, K., Santoso, C., Sheynkman, G., Inukai, S., Kaundal, B., et al. (2024).  
962 Widespread variation in molecular interactions and regulatory properties among  
963 transcription factor isoforms. *bioRxiv*, 2024.03.12.584681. doi:  
964 10.1101/2024.03.12.584681
- 965 Latil, M., Nassar, D., Beck, B., Boumahdi, S., Wang, L., Brisebarre, A., et al. (2017). Cell-Type-  
966 Specific Chromatin States Differentially Prime Squamous Cell Carcinoma Tumor-

- 967 Initiating Cells for Epithelial to Mesenchymal Transition. *Cell Stem Cell* 20, 191-204.e5.  
968 doi: 10.1016/j.stem.2016.10.018
- 969 LeBoeuf, M., Terrell, A., Trivedi, S., Sinha, S., Epstein, J. A., Olson, E. N., et al. (2010). Hdac1  
970 and Hdac2 act redundantly to control p63 and p53 functions in epidermal progenitor  
971 cells. *Dev Cell* 19, 807–818. doi: 10.1016/j.devcel.2010.10.015
- 972 Lecellier, C.-H., Wasserman, W. W., and Mathelier, A. (2018). Human Enhancers Harboring  
973 Specific Sequence Composition, Activity, and Genome Organization Are Linked to the  
974 Immune Response. *Genetics* 209, 1055–1071. doi: 10.1534/genetics.118.301116
- 975 Lena, A. M., Rossi, V., Osterburg, S., Smirnov, A., Osterburg, C., Tuppi, M., et al. (2021). The  
976 p63 C-terminus is essential for murine oocyte integrity. *Nat Commun* 12, 383. doi:  
977 10.1038/s41467-020-20669-0
- 978 Li, H., Handsaker, B., Wysoker, A., Fennell, T., Ruan, J., Homer, N., et al. (2009). The  
979 Sequence Alignment/Map format and SAMtools. *Bioinformatics* 25, 2078–2079. doi:  
980 10.1093/bioinformatics/btp352
- 981 Li, L., Wang, Y., Torkelson, J. L., Shankar, G., Pattison, J. M., Zhen, H. H., et al. (2019).  
982 TFAP2C- and p63-Dependent Networks Sequentially Rearrange Chromatin Landscapes  
983 to Drive Human Epidermal Lineage Commitment. *Cell Stem Cell* 24, 271-284.e8. doi:  
984 10.1016/j.stem.2018.12.012
- 985 Li, Y., Giovannini, S., Wang, T., Fang, J., Li, P., Shao, C., et al. (2023). p63: a crucial player in  
986 epithelial stemness regulation. *Oncogene* 42, 3371–3384. doi: 10.1038/s41388-023-  
987 02859-4
- 988 Lim, F., Solvason, J. J., Ryan, G. E., Le, S. H., Jindal, G. A., Steffen, P., et al. (2024). Affinity-  
989 optimizing enhancer variants disrupt development. *Nature*, 1–9. doi: 10.1038/s41586-  
990 023-06922-8
- 991 Lin-Shiao, E., Lan, Y., Welzenbach, J., Alexander, K. A., Zhang, Z., Knapp, M., et al. (2019).  
992 p63 establishes epithelial enhancers at critical craniofacial development genes. *Science*  
993 *Advances* 5, eaaw0946. doi: 10.1126/sciadv.aaw0946
- 994 Long, H. K., Prescott, S. L., and Wysocka, J. (2016). Ever-Changing Landscapes:  
995 Transcriptional Enhancers in Development and Evolution. *Cell* 167, 1170–1187. doi:  
996 10.1016/j.cell.2016.09.018
- 997 Lopez-Pajares, V., Qu, K., Zhang, J., Webster, D. E., Barajas, B. C., Siprashvili, Z., et al.  
998 (2015). A LncRNA-MAF:MAFB Transcription Factor Network Regulates Epidermal  
999 Differentiation. *Developmental Cell* 32, 693–706. doi: 10.1016/j.devcel.2015.01.028
- 1000 Marshall, C. B., Beeler, J. S., Lehmann, B. D., Gonzalez-Ericsson, P., Sanchez, V., Sanders, M.  
1001 E., et al. (2021). Tissue-specific expression of p73 and p63 isoforms in human tissues.  
1002 *Cell Death Dis* 12, 1–10. doi: 10.1038/s41419-021-04017-8
- 1003 Massion, P. P., Taflan, P. M., Jamshedur Rahman, S. M., Yildiz, P., Shyr, Y., Edgerton, M. E.,  
1004 et al. (2003). Significance of p63 amplification and overexpression in lung cancer  
1005 development and prognosis. *Cancer Res* 63, 7113–7121.
- 1006 McDade, S. S., Henry, A. E., Pivato, G. P., Kozarewa, I., Mitsopoulos, C., Fenwick, K., et al.  
1007 (2012). Genome-wide analysis of p63 binding sites identifies AP-2 factors as co-  
1008 regulators of epidermal differentiation. *Nucleic Acids Res* 40, 7190–7206. doi:  
1009 10.1093/nar/gks389
- 1010 McGrath, J. A., Duijf, P. H. G., Doetsch, V., Irvine, A. D., Waal, R. de, Vanmolkot, K. R. J., et al.  
1011 (2001). Hay–Wells syndrome is caused by heterozygous missense mutations in the  
1012 SAM domain of p63. *Human Molecular Genetics* 10, 221–230. doi:  
1013 10.1093/hmg/10.3.221
- 1014 Melino, G., Memmi, E. M., Pelicci, P. G., and Bernassola, F. (2015). Maintaining epithelial  
1015 stemness with p63. *Sci. Signal.* 8, re9–re9. doi: 10.1126/scisignal.aaa1033
- 1016 Mills, A. A., Zheng, B., Wang, X. J., Vogel, H., Roop, D. R., and Bradley, A. (1999). p63 is a p53  
1017 homologue required for limb and epidermal morphogenesis. *Nature* 398, 708–13. doi:

- 1018 10.1038/19531
- 1019 Moore, J. E., Purcaro, M. J., Pratt, H. E., Epstein, C. B., Shores, N., Adrian, J., et al. (2020).
- 1020 Expanded encyclopaedias of DNA elements in the human and mouse genomes. *Nature*
- 1021 583, 699–710. doi: 10.1038/s41586-020-2493-4
- 1022 Moses, M. A., George, A. L., Sakakibara, N., Mahmood, K., Ponnamperuma, R. M., King, K. E.,
- 1023 et al. (2019). Molecular Mechanisms of p63-Mediated Squamous Cancer Pathogenesis.
- 1024 *Int J Mol Sci* 20, 3590. doi: 10.3390/ijms20143590
- 1025 Muerdter, F., Boryń, Ł. M., Woodfin, A. R., Neumayr, C., Rath, M., Zabidi, M. A., et al. (2018).
- 1026 Resolving systematic errors in widely used enhancer activity assays in human cells. *Nat*
- 1027 *Methods* 15, 141–149. doi: 10.1038/nmeth.4534
- 1028 Murray-Zmijewski, F., Lane, D. P., and Bourdon, J.-C. (2006). p53/p63/p73 isoforms: an
- 1029 orchestra of isoforms to harmonise cell differentiation and response to stress. *Cell Death*
- 1030 *Differ* 13, 962–972. doi: 10.1038/sj.cdd.4401914
- 1031 Napoli, M., Deshpande, A. A., Chakravarti, D., Rajapakshe, K., Gunaratne, P. H., Coarfa, C., et
- 1032 al. (2024). Genome-wide p63-Target Gene Analyses Reveal TAp63/NRF2-Dependent
- 1033 Oxidative Stress Responses. *Cancer Research Communications* 4, 264–278. doi:
- 1034 10.1158/2767-9764.CRC-23-0358
- 1035 Neumayr, C., Haberle, V., Serebreni, L., Karner, K., Hendy, O., Boija, A., et al. (2022).
- 1036 Differential cofactor dependencies define distinct types of human enhancers. *Nature*, 1–
- 1037 8. doi: 10.1038/s41586-022-04779-x
- 1038 Ng, S. Y., Yoshida, N., Christie, A. L., Ghandi, M., Dharia, N. V., Dempster, J., et al. (2018).
- 1039 Targetable vulnerabilities in T- and NK-cell lymphomas identified through preclinical
- 1040 models. *Nat Commun* 9, 2024. doi: 10.1038/s41467-018-04356-9
- 1041 Osterburg, C., and Dötsch, V. (2022). Structural diversity of p63 and p73 isoforms. *Cell Death*
- 1042 *Differ* 29, 921–937. doi: 10.1038/s41418-022-00975-4
- 1043 Pastushenko, I., and Blanpain, C. (2019). EMT Transition States during Tumor Progression and
- 1044 Metastasis. *Trends in Cell Biology* 29, 212–226. doi: 10.1016/j.tcb.2018.12.001
- 1045 Pattison, J. M., Melo, S. P., Piekos, S. N., Torkelson, J. L., Bashkurova, E., Mumbach, M. R., et
- 1046 al. (2018). Retinoic acid and BMP4 cooperate with p63 to alter chromatin dynamics
- 1047 during surface epithelial commitment. *Nat Genet* 50, 1658–1665. doi: 10.1038/s41588-
- 1048 018-0263-0
- 1049 Peinado, H., Olmeda, D., and Cano, A. (2007). Snail, Zeb and bHLH factors in tumour
- 1050 progression: an alliance against the epithelial phenotype? *Nat Rev Cancer* 7, 415–428.
- 1051 doi: 10.1038/nrc2131
- 1052 Peng, T., Zhai, Y., Atlasi, Y., ter Huurne, M., Marks, H., Stunnenberg, H. G., et al. (2020).
- 1053 STARR-seq identifies active, chromatin-masked, and dormant enhancers in pluripotent
- 1054 mouse embryonic stem cells. *Genome Biology* 21, 243. doi: 10.1186/s13059-020-02156-
- 1055 3
- 1056 Perez, C. A., Ott, J., Mays, D. J., and Pietenpol, J. A. (2007). p63 consensus DNA-binding site:
- 1057 identification, analysis and application into a p63MH algorithm. *Oncogene* 26, 7363–
- 1058 7370. doi: 10.1038/sj.onc.1210561
- 1059 Pickering, C. R., Zhou, J. H., Lee, J. J., Drummond, J. A., Peng, S. A., Saade, R. E., et al.
- 1060 (2014). Mutational landscape of aggressive cutaneous squamous cell carcinoma. *Clin*
- 1061 *Cancer Res* 20, 6582–92. doi: 10.1158/1078-0432.CCR-14-1768
- 1062 Pokorna, Z., Vyslouzil, J., Vojtesek, B., and Coates, P. J. (2022). Identifying pathways
- 1063 regulating the oncogenic p53 family member  $\Delta$ Np63 provides therapeutic avenues for
- 1064 squamous cell carcinoma. *Cell Mol Biol Lett* 27, 18. doi: 10.1186/s11658-022-00323-x
- 1065 Qu, J., Tanis, S. E. J., Smits, J. P. H., Kouwenhoven, E. N., Oti, M., Van Den Bogaard, E. H., et
- 1066 al. (2018). Mutant p63 Affects Epidermal Cell Identity through Rewiring the Enhancer
- 1067 Landscape. *Cell Reports* 25, 3490–3503.e4. doi: 10.1016/j.celrep.2018.11.039
- 1068 Qu, J., Yi, G., and Zhou, H. (2019). p63 cooperates with CTCF to modulate chromatin

- 1069 architecture in skin keratinocytes. *Epigenetics Chromatin* 12, 31. doi: 10.1186/s13072-  
1070 019-0280-y
- 1071 Quinlan, A. R., and Hall, I. M. (2010). BEDTools: a flexible suite of utilities for comparing  
1072 genomic features. *Bioinformatics* 26, 841–842. doi: 10.1093/bioinformatics/btq033
- 1073 Rahimov, F., Marazita, M. L., Visel, A., Cooper, M. E., Hitchler, M. J., Rubini, M., et al. (2008).  
1074 Disruption of an AP-2alpha binding site in an IRF6 enhancer is associated with cleft lip.  
1075 *Nat. Genet.* 40, 1341–1347. doi: 10.1038/ng.242
- 1076 Ramírez, F., Ryan, D. P., Grüning, B., Bhardwaj, V., Kilpert, F., Richter, A. S., et al. (2016).  
1077 deepTools2: a next generation web server for deep-sequencing data analysis. *Nucleic  
1078 Acids Res* 44, W160–W165. doi: 10.1093/nar/gkw257
- 1079 Ramsey, M. R., He, L., Forster, N., Ory, B., and Ellisen, L. W. (2011). Physical association of  
1080 HDAC1 and HDAC2 with p63 mediates transcriptional repression and tumor  
1081 maintenance in squamous cell carcinoma. *Cancer Res* 71, 4373–4379. doi:  
1082 10.1158/0008-5472.CAN-11-0046
- 1083 Ramsey, M. R., Wilson, C., Ory, B., Rothenberg, S. M., Faquin, W., Mills, A. A., et al. (2013).  
1084 FGFR2 signaling underlies p63 oncogenic function in squamous cell carcinoma. *J Clin  
1085 Invest* 123, 3525–3538. doi: 10.1172/JCI68899
- 1086 Ricci-Tam, C., Ben-Zion, I., Wang, J., Palme, J., Li, A., Savir, Y., et al. (2021). Decoupling  
1087 transcription factor expression and activity enables dimmer switch gene regulation.  
1088 *Science* 372, 292–295. doi: 10.1126/science.aba7582
- 1089 Richardson, R., Mitchell, K., Hammond, N. L., Mollo, M. R., Kouwenhoven, E. N., Wyatt, N. D.,  
1090 et al. (2017). p63 exerts spatio-temporal control of palatal epithelial cell fate to prevent  
1091 cleft palate. *PLoS Genet.* 13, e1006828. doi: 10.1371/journal.pgen.1006828
- 1092 Riege, K., Kretzmer, H., Sahm, A., McDade, S. S., Hoffmann, S., and Fischer, M. (2020).  
1093 Dissecting the DNA binding landscape and gene regulatory network of p63 and p53.  
1094 *eLife* 9, e63266. doi: 10.7554/eLife.63266
- 1095 Safieh, J., Chazan, A., Saleem, H., Vyas, P., Danin-Poleg, Y., Ron, D., et al. (2023). A  
1096 molecular mechanism for the “digital” response of p53 to stress. *Proceedings of the  
1097 National Academy of Sciences* 120, e2305713120. doi: 10.1073/pnas.2305713120
- 1098 Sahu, B., Hartonen, T., Pihlajamaa, P., Wei, B., Dave, K., Zhu, F., et al. (2022). Sequence  
1099 determinants of human gene regulatory elements. *Nat Genet*, 1–12. doi:  
1100 10.1038/s41588-021-01009-4
- 1101 Saladi, S. V., Ross, K., Karaayvaz, M., Tata, P. R., Mou, H., Rajagopal, J., et al. (2017).  
1102 ACTL6A Is Co-Amplified with p63 in Squamous Cell Carcinoma to Drive YAP Activation,  
1103 Regenerative Proliferation, and Poor Prognosis. *Cancer Cell* 31, 35–49. doi:  
1104 10.1016/j.ccell.2016.12.001
- 1105 Santos-Pereira, J. M., Gallardo-Fuentes, L., Neto, A., Acemel, R. D., and Tena, J. J. (2019).  
1106 Pioneer and repressive functions of p63 during zebrafish embryonic ectoderm  
1107 specification. *Nat Commun* 10, 3049. doi: 10.1038/s41467-019-11121-z
- 1108 Senitzki, A., Safieh, J., Sharma, V., Golovenko, D., Danin-Poleg, Y., Inga, A., et al. (2021). The  
1109 complex architecture of p53 binding sites. *Nucleic Acids Research* 49, 1364–1382. doi:  
1110 10.1093/nar/gkaa1283
- 1111 Senoo, M., Pinto, F., Crum, C. P., and McKeon, F. (2007). p63 Is Essential for the Proliferative  
1112 Potential of Stem Cells in Stratified Epithelia. *Cell* 129, 523–536. doi:  
1113 10.1016/j.cell.2007.02.045
- 1114 Seo, J., Koçak, D. D., Bartelt, L. C., Williams, C. A., Barrera, A., Gersbach, C. A., et al. (2021).  
1115 AP-1 subunits converge promiscuously at enhancers to potentiate transcription. *Genome  
1116 Res.* 31, 538–550. doi: 10.1101/gr.267898.120
- 1117 Sethi, I., Gluck, C., Zhou, H., Buck, M. J., and Sinha, S. (2017). Evolutionary re-wiring of p63  
1118 and the epigenomic regulatory landscape in keratinocytes and its potential implications  
1119 on species-specific gene expression and phenotypes. *Nucleic Acids Research* 45,

- 1120 8208–8224. doi: 10.1093/nar/gkx416
- 1121 Sethi, I., Romano, R.-A., Gluck, C., Smalley, K., Vojtesek, B., Buck, M. J., et al. (2015). A global  
1122 analysis of the complex landscape of isoforms and regulatory networks of p63 in human  
1123 cells and tissues. *BMC Genomics* 16, 584. doi: 10.1186/s12864-015-1793-9
- 1124 Sethi, I., Sinha, S., and Buck, M. J. (2014). Role of chromatin and transcriptional co-regulators  
1125 in mediating p63-genome interactions in keratinocytes. *BMC Genomics* 15, 1042. doi:  
1126 10.1186/1471-2164-15-1042
- 1127 Sheffield, N. C., Thurman, R. E., Song, L., Safi, A., Stamatoyannopoulos, J. A., Lenhard, B., et  
1128 al. (2013). Patterns of regulatory activity across diverse human cell types predict tissue  
1129 identity, transcription factor binding, and long-range interactions. *Genome Res.* 23, 777–  
1130 788. doi: 10.1101/gr.152140.112
- 1131 Slattery, M., Zhou, T., Yang, L., Dantas Machado, A. C., Gordân, R., and Rohs, R. (2014).  
1132 Absence of a simple code: how transcription factors read the genome. *Trends in*  
1133 *Biochemical Sciences* 39, 381–399. doi: 10.1016/j.tibs.2014.07.002
- 1134 Song, E.-A. C., Min, S., Oyelakin, A., Smalley, K., Bard, J. E., Liao, L., et al. (2018). Genetic and  
1135 scRNA-seq Analysis Reveals Distinct Cell Populations that Contribute to Salivary Gland  
1136 Development and Maintenance. *Sci Rep* 8, 14043. doi: 10.1038/s41598-018-32343-z
- 1137 Spitz, F., and Furlong, E. E. M. (2012). Transcription factors: from enhancer binding to  
1138 developmental control. *Nat Rev Genet* 13, 613–626. doi: 10.1038/nrg3207
- 1139 Strubel, A., Münick, P., Hartmann, O., Chaikuad, A., Dreier, B., Schaefer, J. V., et al. (2023).  
1140 DARPinS detect the formation of hetero-tetramers of p63 and p73 in epithelial tissues  
1141 and in squamous cell carcinoma. *Cell Death Dis* 14, 1–12. doi: 10.1038/s41419-023-  
1142 06213-0
- 1143 Su, X., Paris, M., Gi, Y. J., Tsai, K. Y., Cho, M. S., Lin, Y.-L., et al. (2009). TAp63 prevents  
1144 premature aging by promoting adult stem cell maintenance. *Cell Stem Cell* 5, 64–75. doi:  
1145 10.1016/j.stem.2009.04.003
- 1146 Sundqvist, A., Vasilaki, E., Voytyuk, O., Bai, Y., Morikawa, M., Moustakas, A., et al. (2020).  
1147 TGF $\beta$  and EGF signaling orchestrates the AP-1- and p63 transcriptional regulation of  
1148 breast cancer invasiveness. *Oncogene* 39, 4436–4449. doi: 10.1038/s41388-020-1299-z
- 1149 Szak, S. T., Mays, D., and Pietenpol, J. A. (2001). Kinetics of p53 Binding to Promoter Sites In  
1150 Vivo. *Molecular and Cellular Biology* 21, 3375–3386. doi: 10.1128/MCB.21.10.3375-  
1151 3386.2001
- 1152 Taskiran, I. I., Spanier, K. I., Dickmänken, H., Kempynck, N., Pančiková, A., Ekşi, E. C., et al.  
1153 (2024). Cell-type-directed design of synthetic enhancers. *Nature* 626, 212–220. doi:  
1154 10.1038/s41586-023-06936-2
- 1155 Thomason, H. A., Zhou, H., Kouwenhoven, E. N., Dotto, G.-P., Restivo, G., Nguyen, B.-C., et al.  
1156 (2010). Cooperation between the transcription factors p63 and IRF6 is essential to  
1157 prevent cleft palate in mice. *J Clin Invest* 120, 1561–1569. doi: 10.1172/JCI40266
- 1158 Thurfjell, N., Coates, P. J., Vojtesek, B., Benham-Motlagh, P., Eisold, M., and Nylander, K.  
1159 (2005). Endogenous p63 acts as a survival factor for tumour cells of SCCHN origin. *Int J*  
1160 *Mol Med* 16, 1065–1070.
- 1161 Thurman, R. E., Rynes, E., Humbert, R., Vierstra, J., Maurano, M. T., Haugen, E., et al. (2012).  
1162 The accessible chromatin landscape of the human genome. *Nature* 489, 75–82. doi:  
1163 10.1038/nature11232
- 1164 Trauernicht, M., Martinez-Ara, M., and Steensel, B. van (2020). Deciphering Gene Regulation  
1165 Using Massively Parallel Reporter Assays. *Trends in Biochemical Sciences* 45, 90–91.  
1166 doi: 10.1016/j.tibs.2019.10.006
- 1167 Trauernicht, M., Rastogi, C., Manzo, S. G., Bussemaker, H. J., and van Steensel, B. (2023).  
1168 Optimisation of TP53 reporters by systematic dissection of synthetic TP53 response  
1169 elements. *Nucleic Acids Res* 51, 9690–9702. doi: 10.1093/nar/gkad718
- 1170 Truong, A. B., Kretz, M., Ridky, T. W., Kimmel, R., and Khavari, P. A. (2006). p63 regulates

- 1171 proliferation and differentiation of developmentally mature keratinocytes. *Genes Dev.* 20,  
1172 3185–3197. doi: 10.1101/gad.1463206
- 1173 Tucci, P., Agostini, M., Grespi, F., Markert, E. K., Terrinoni, A., Vousden, K. H., et al. (2012).  
1174 Loss of p63 and its microRNA-205 target results in enhanced cell migration and  
1175 metastasis in prostate cancer. *Proceedings of the National Academy of Sciences* 109,  
1176 15312–15317. doi: 10.1073/pnas.1110977109
- 1177 van Bokhoven, H., Hamel, B. C. J., Bamshad, M., Sangiorgi, E., Gurrieri, F., Duijf, P. H. G., et  
1178 al. (2001). p63 Gene Mutations in EEC Syndrome, Limb-Mammary Syndrome, and  
1179 Isolated Split Hand–Split Foot Malformation Suggest a Genotype-Phenotype Correlation.  
1180 *The American Journal of Human Genetics* 69, 481–492. doi: 10.1086/323123
- 1181 Verfaillie, A., Svetlichnyy, D., Imrichova, H., Davie, K., Fiers, M., Atak, Z. K., et al. (2016).  
1182 Multiplex enhancer-reporter assays uncover unsophisticated TP53 enhancer logic.  
1183 *Genome Res.* 26, 882–895. doi: 10.1101/gr.204149.116
- 1184 Vu, H., and Ernst, J. (2022). Universal annotation of the human genome through integration of  
1185 over a thousand epigenomic datasets. *Genome Biology* 23, 9. doi: 10.1186/s13059-021-  
1186 02572-z
- 1187 Wang, E. T., Sandberg, R., Luo, S., Khrebtkova, I., Zhang, L., Mayr, C., et al. (2008).  
1188 Alternative isoform regulation in human tissue transcriptomes. *Nature* 456, 470–476. doi:  
1189 10.1038/nature07509
- 1190 White, M. A., Myers, C. A., Corbo, J. C., and Cohen, B. A. (2013). Massively parallel in vivo  
1191 enhancer assay reveals that highly local features determine the cis-regulatory function of  
1192 ChIP-seq peaks. *Proceedings of the National Academy of Sciences* 110, 11952–11957.  
1193 doi: 10.1073/pnas.1307449110
- 1194 Wilson, V. G. (2013). “Growth and Differentiation of HaCaT Keratinocytes,” in *Epidermal Cells*,  
1195 ed. K. Turksen (New York, NY: Springer New York), 33–41. doi: 10.1007/7651\_2013\_42
- 1196 Woodstock, D. L., Sammons, M. A., and Fischer, M. (2021). p63 and p53: Collaborative  
1197 Partners or Dueling Rivals? *Frontiers in Cell and Developmental Biology* 9. Available at:  
1198 <https://www.frontiersin.org/articles/10.3389/fcell.2021.701986> (Accessed September 14,  
1199 2022).
- 1200 Wu, G., Yoshida, N., Liu, J., Zhang, X., Xiong, Y., Heavican-Foral, T. B., et al. (2023). TP63  
1201 fusions drive multicomplex enhancer rewiring, lymphomagenesis, and EZH2  
1202 dependence. *Science Translational Medicine* 15, eadi7244. doi:  
1203 10.1126/scitranslmed.adi7244
- 1204 Yallowitz, A. R., Alexandrova, E. M., Talos, F., Xu, S., Marchenko, N. D., and Moll, U. M. (2014).  
1205 p63 is a prosurvival factor in the adult mammary gland during post-lactational involution,  
1206 affecting PI-MECs and ErbB2 tumorigenesis. *Cell Death Differ* 21, 645–654. doi:  
1207 10.1038/cdd.2013.199
- 1208 Yanez-Cuna, J. O., Dinh, H. Q., Kvon, E. Z., Shlyueva, D., and Stark, A. (2012). Uncovering cis-  
1209 regulatory sequence requirements for context-specific transcription factor binding.  
1210 *Genome Res* 22, 2018–30. doi: 10.1101/gr.132811.111
- 1211 Yang, A., Kaghad, M., Wang, Y., Gillett, E., Fleming, M. D., Dötsch, V., et al. (1998). p63, a p53  
1212 Homolog at 3q27–29, Encodes Multiple Products with Transactivating, Death-Inducing,  
1213 and Dominant-Negative Activities. *Molecular Cell* 2, 305–316. doi: 10.1016/S1097-  
1214 2765(00)80275-0
- 1215 Yang, A., Zhu, Z., Kapranov, P., McKeon, F., Church, G. M., Gingeras, T. R., et al. (2006).  
1216 Relationships between p63 Binding, DNA Sequence, Transcription Activity, and  
1217 Biological Function in Human Cells. *Molecular Cell* 24, 593–602. doi:  
1218 10.1016/j.molcel.2006.10.018
- 1219 Yoh, K. E., Regunath, K., Guzman, A., Lee, S.-M., Pfister, N. T., Akanni, O., et al. (2016).  
1220 Repression of p63 and induction of EMT by mutant Ras in mammary epithelial cells.  
1221 *Proceedings of the National Academy of Sciences* 113, E6107–E6116. doi:

1222 10.1073/pnas.1613417113  
1223 Yu, X., Singh, P. K., Tabrejje, S., Sinha, S., and Buck, M. J. (2021).  $\Delta$ Np63 is a pioneer factor  
1224 that binds inaccessible chromatin and elicits chromatin remodeling. *Epigenetics &*  
1225 *Chromatin* 14, 20. doi: 10.1186/s13072-021-00394-8  
1226 Zaret, K. S., and Mango, S. E. (2016). Pioneer transcription factors, chromatin dynamics, and  
1227 cell fate control. *Curr Opin Genet Dev* 37, 76–81. doi: 10.1016/j.gde.2015.12.003

# Figure 1

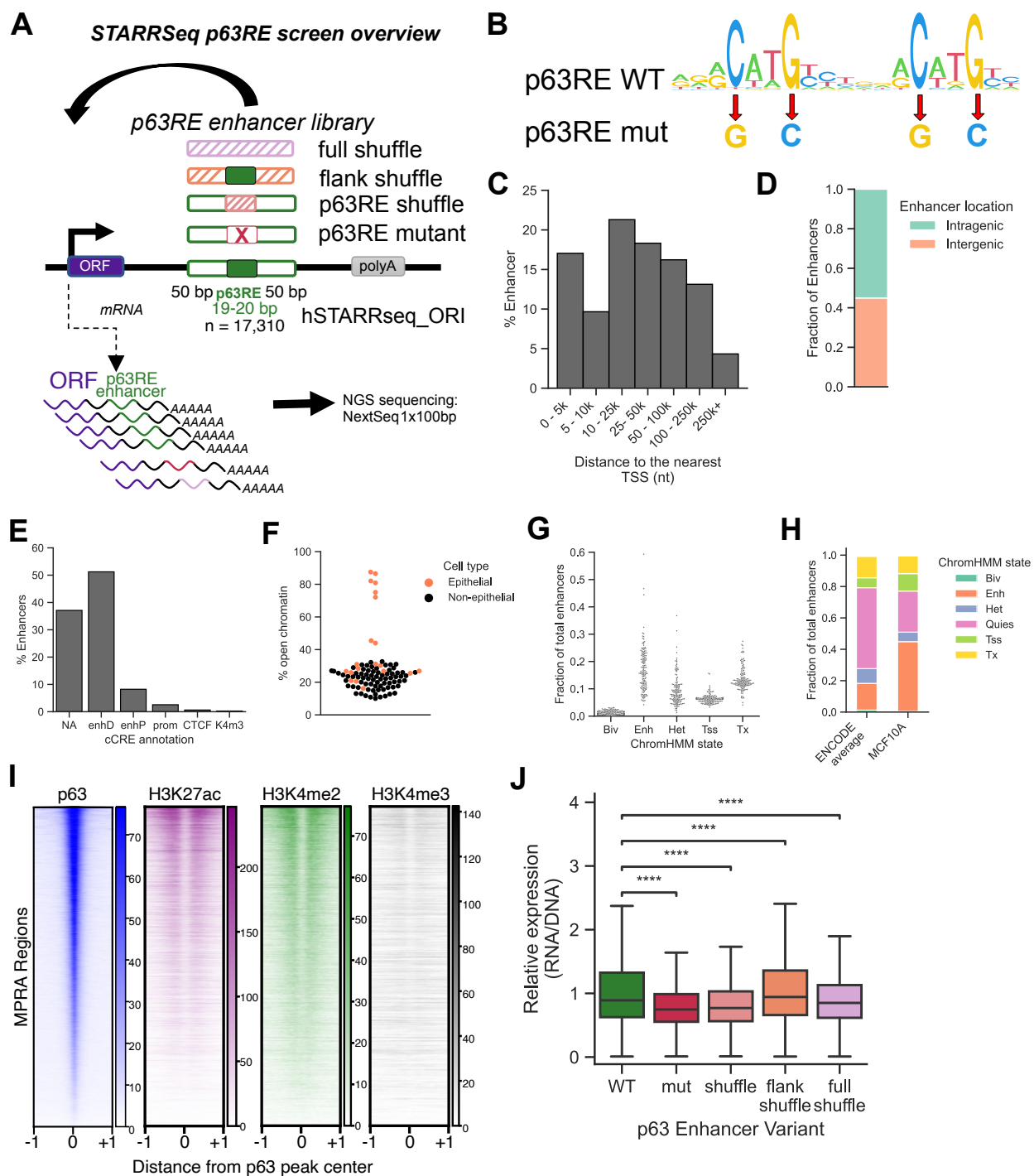


## Figure 2

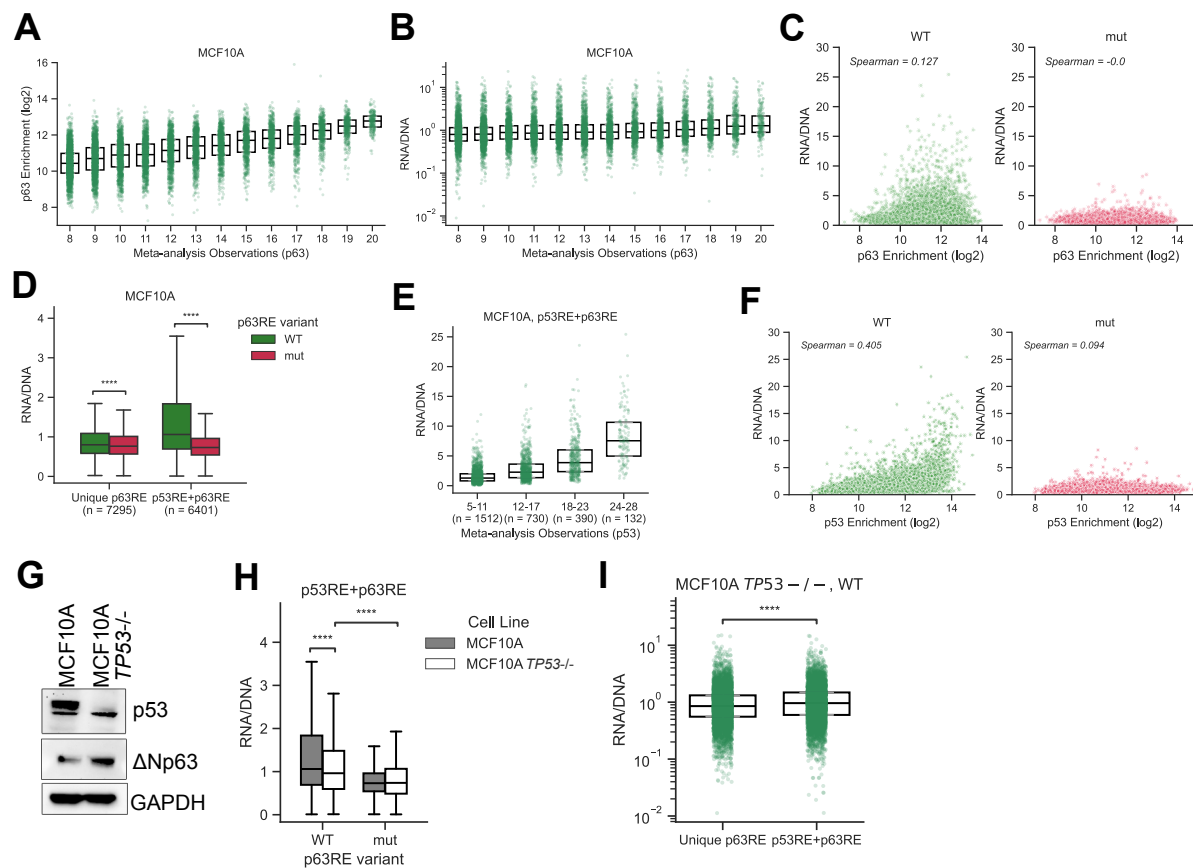


# Figure 3

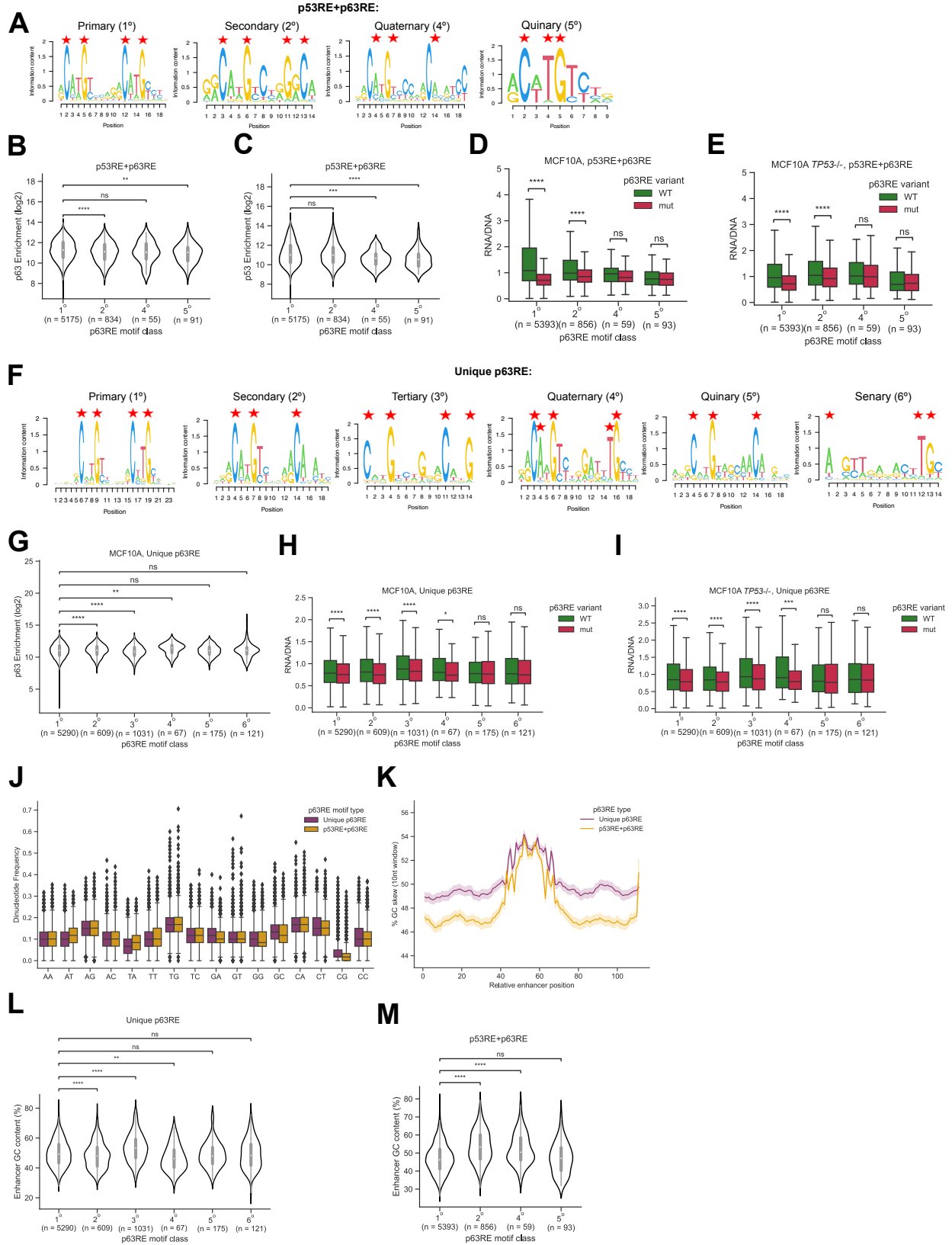


## Figure 4

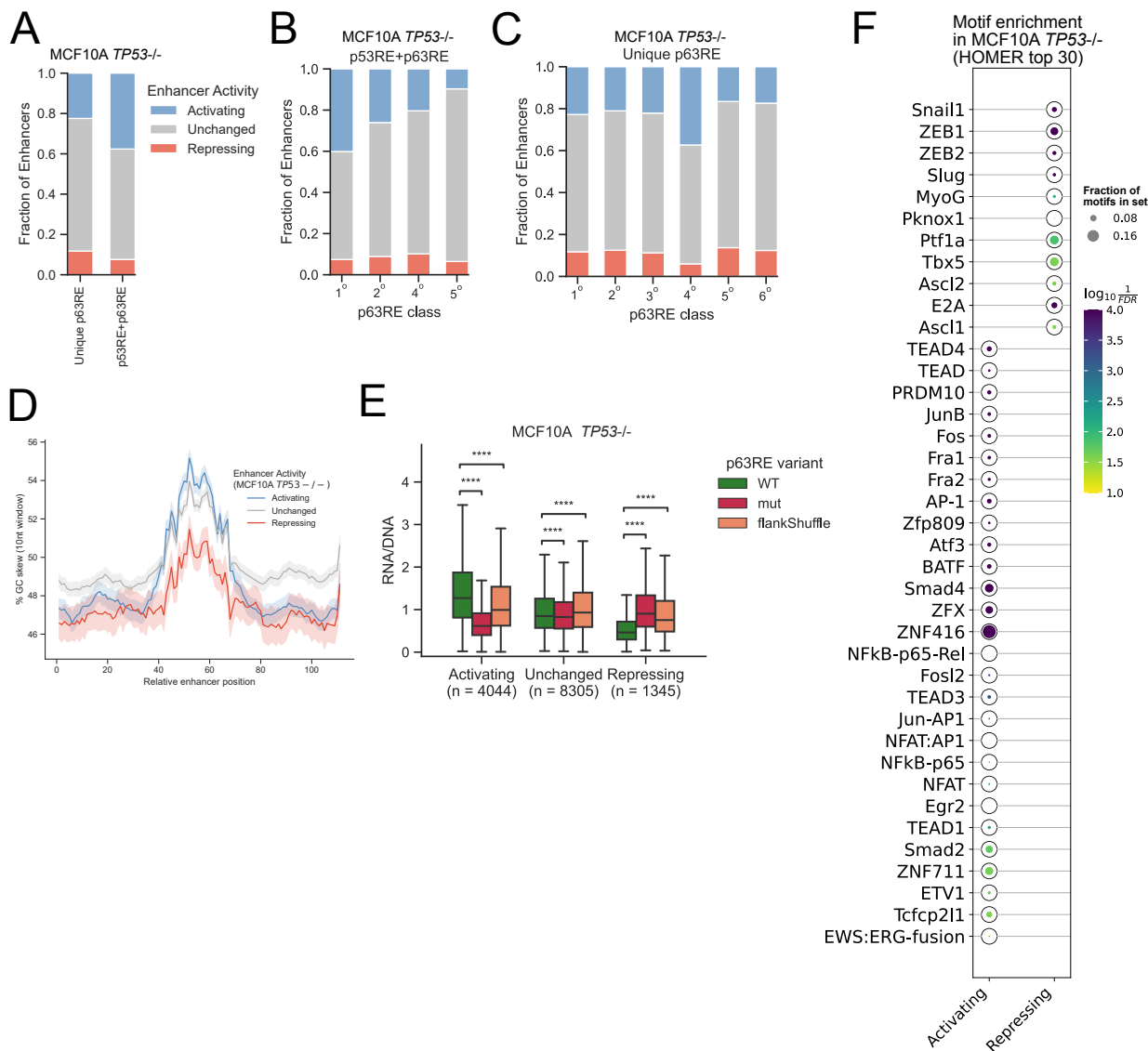


# Figure 5

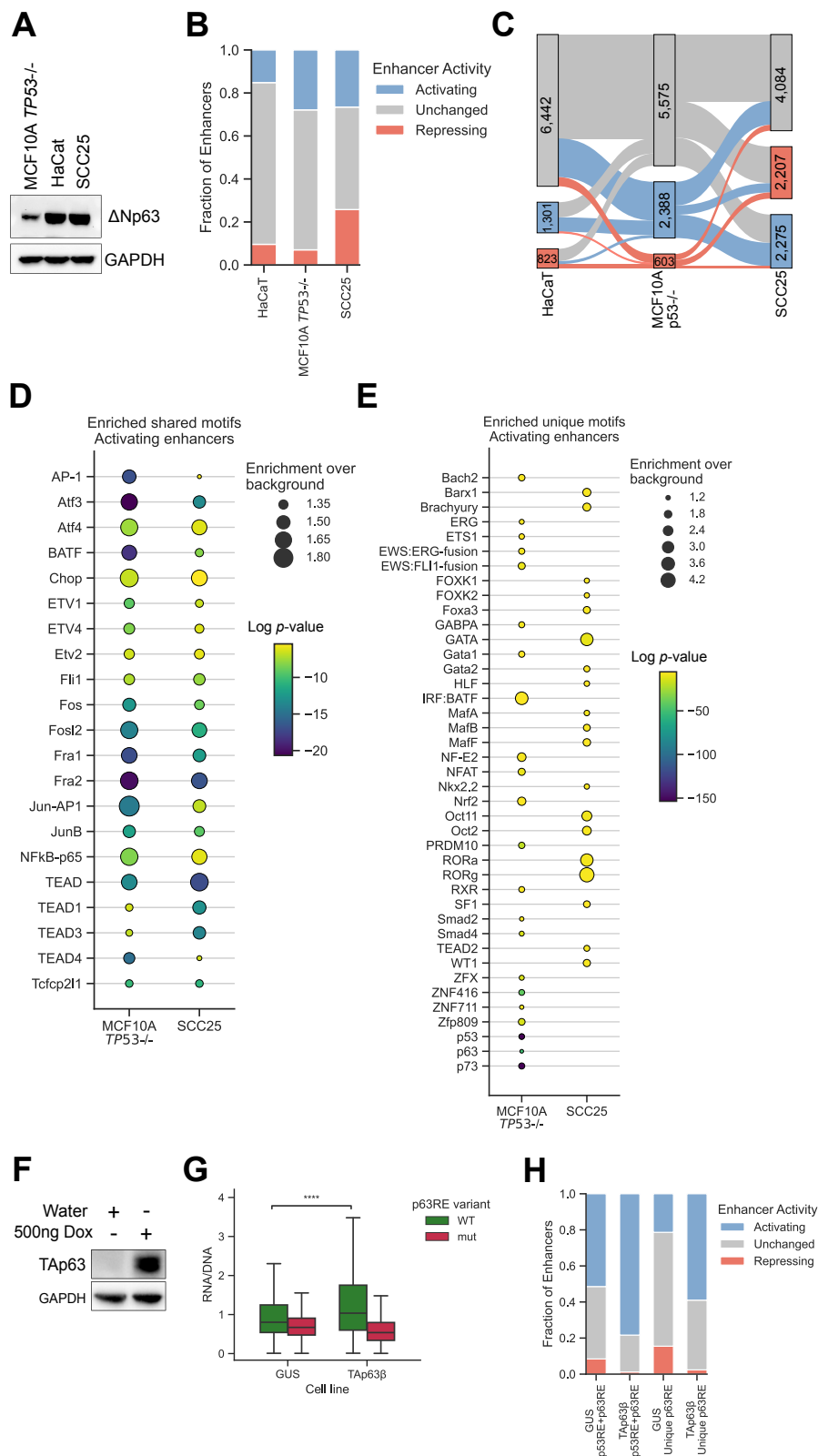
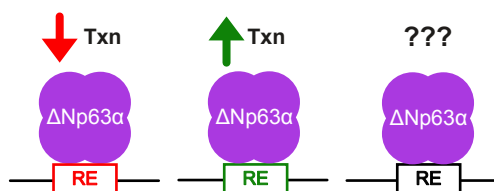


## Figure 6

A



B

